Journal of Surgical Oncology 2014;109:189–197

TNK2 Gene Amplification is a Novel Predictor of a Poor Prognosis in Patients With Gastric Cancer

KAZUYA SHINMURA, MD, PhD,[1]* SHINICHIRO KIYOSE, BS,[1] KIYOKO NAGURA, BS,[1] HISAKI IGARASHI, BS,[1] YUSUKE INOUE, MD,[1] SATOKI NAKAMURA, MD, PhD,[1] MATSUYOSHI MAEDA, MD, PhD,[2] MEGUMI BABA, MD, PhD,[3] HIROYUKI KONNO, MD, PhD,[3] AND HARUHIKO SUGIMURA, MD, PhD[1]

[1]*Department of Tumor Pathology, Hamamatsu University School of Medicine, Hamamatsu, Japan*
[2]*Department of Pathology, Toyohashi Municipal Hospital, Toyohashi, Japan*
[3]*Department of Surgery 2, Hamamatsu University School of Medicine, Hamamatsu, Japan*

Backgrounds and Objectives: We previously examined the amplification status of 10 kinase genes (*PIK3CA*, *EPHB3*, *TNK2*, *PTK7*, *EGFR*, *MET*, *ERBB2*, *HCK*, *SRC*, and *AURKA*) in gastric cancer (GC). This study aimed to determine the prognostic significance of these gene amplifications in GC.

Methods: A survival analysis was performed for GC patients. Since *TNK2* amplification was identified as a prognostic marker in the analysis, we also examined the functional effect of TNK2 overexpression on gastric cells.

Results: A Kaplan–Meier analysis showed that the prognosis of patients with GC exhibiting *TNK2* or *AURKA* amplification was significantly poorer than the prognosis of patients with GC without *TNK2* or *AURKA* amplification. A further multivariate analysis revealed that *TNK2* amplification was an independent predictor of a poor survival outcome among patients with GC (hazard ratio, 3.668; 95% confidence interval, 1.513–7.968; $P = 0.0056$). TNK2-overexpressing GC cells showed an increase in cell migration and non-anchored cell growth. Finally, microarray and pathway analyses revealed the aberrant regulation of some cancer-related pathways in TNK2-overexpressing GC cells.

Conclusions: These results suggested that *TNK2* amplification is an independent predictor of a poor prognosis in patients with GC and leads to an increase in the malignant potential of GC cells.

J. Surg. Oncol. 2014;109:189–197.

KEY WORDS: **gastric cancer; gene amplification; prognostic marker; survival analysis; TNK2**

INTRODUCTION

TNK2 (also known as Ack1) is a non-receptor tyrosine kinase consisting of a sterile α-motif domain, a tyrosine kinase domain, an SH3 domain, a Cdc42/Rac interactive binding domain, proline-rich sequences, and an ubiquitin association domain [1,2]. TNK2 is ubiquitously expressed in humans [3] and senses extracellular signals by interacting with membrane-bound activated receptor-tyrosine kinases such as EGFR, HER2, ALK, and MERTK [3–6]. Such interactions result in not only TNK2 activation, but also signal transduction through the activation of various downstream effector proteins, such as Cdc42, AKT, androgen receptor (AR), and Wwox [1,4,7–9]. Through these TNK2-signaling networks, TNK2 participates in survival, migration, and tumorigenesis [2].

The *TNK2* gene is amplified in various human carcinomas including lung, ovarian, gastric, and prostate cancer, and *TNK2* gene amplification leads to an elevated mRNA transcript level [10,11]. TNK2 overexpression causes increases in metastasis and mortality in a mouse model, and TNK2 is involved in an extracellular matrix-induced integrin signal, resulting in the activation of signaling processes such as the activation of the small GTPase Rac [10]. However, whether *TNK2* amplification is a prognostic factor in human cancer has not yet been reported.

We recently examined the amplification status of 100 kinase genes using a fluorescence in situ hybridization (FISH) analysis with a tissue microarray (TMA) containing a total of 60 carcinomas, consisting of colorectal, lung, and gastric carcinomas [11]. We then selected 10 kinases (*PIK3CA*, *EPHB3*, *TNK2*, *PTK7*, *EGFR*, *MET*, *ERBB2*, *HCK*, *SRC*, and *AURKA*) for which genomic amplification was detected at a frequency of 5% or more and examined the amplification status of these genes in more than 300 gastric cancers (GCs) [12]. Since gene amplification in cancer can sometimes define the prognosis of cancer patients [13–16], in the present study, we tested whether the amplification of the 10 above-mentioned genes was capable of predicting the prognosis of patients with GC and found that *TNK2* amplification independently predicts a poor survival among patients with GC. Then, to investigate the underlying mechanism, we also examined the effect of TNK2 overexpression on gastric cells.

Abbreviations: BAC, bacterial artificial chromosome; FISH, fluorescence in situ hybridization; GC, gastric cancer; TMA, tissue microarray.

Grant sponsor: Ministry of Health, Labour and Welfare;
Grant number: 21-1; Grant sponsor: Japan Society for the Promotion of Science;
Grant number: 25460476; Grant sponsor: Ministry of Education, Culture, Sports, Science and Technology;
Grant number: 221S0001

*Correspondence to: Kazuya Shinmura, MD, PhD, Department of Tumor Pathology, Hamamatsu University School of Medicine, 1-20-1 Handayama, Higashi Ward, Hamamatsu, Shizuoka 431-3192, Japan. Fax: +81-53-435-2225. E-mail: kzshinmu@hama-med.ac.jp

Received 31 July 2013; Accepted 10 October 2013

DOI 10.1002/jso.23482

Published online 31 October 2013 in Wiley Online Library (wileyonlinelibrary.com).

MATERIALS AND METHODS

Cell Line and Primary Carcinomas

A GC cell line AGS was obtained from the American Type Culture Collection (Manassas, VA). The AGS cells and their derivatives were maintained at 37°C in RPMI1640 medium supplemented with 10% fetal bovine serum (Equitech-Bio, Kerrville, TX) and penicillin/streptomycin under a 5% CO_2 atmosphere. GC tissues from two groups of primary GC patients (n = 271 and n = 335) were obtained from the Toyohashi Municipal Hospital (Japan) and the Hamamatsu University Hospital (Japan), respectively. The study design was approved by the institutional review board.

Preparation of TMA Blocks

A TMA block was prepared by transferring a cylinder with a diameter of 3 mm from each paraffin-embedded tissue sample using a microarrayer (KIN-1; Azumaya, Tokyo, Japan). The histopathological diagnosis of gastric cancer was confirmed by three pathologists (K.S., M.M., and H.S.).

FISH Analysis

TMA sections were de-waxed and re-hydrated, then boiled in 0.01 M citrate buffer (pH 6.0) to release the closed chromosomal structures. A combination of Cy3-labeled bacterial artificial chromosome (BAC) clone (RP11-436M6) for the *TNK2* locus (Advanced GenoTechs Co., Tsukuba, Japan) and a Spectrum Green-labeled control probe for the near centromere locus on chromosome 3 (BAC clone: RP11-91A15) or a combination of Cy3-labeled BAC clone (RP11-65K20) for the *AURKA* locus (Advanced GenoTechs Co.) and a Spectrum Green-labeled control probe for the near centromere locus on chromosome 20 (BAC clone: RP11-32N12) were placed on a slide and covered with a coverslip. The slides with the hybridization mixture were denatured on a digital hot plate (HP-15; AS ONE Corp., Osaka, Japan) and then incubated overnight at 42°C. After washing the slide in 50% formamide/2X SSC, mounting medium containing DAPI (Vector Laboratories, Burlingame, CA) was used for nuclear counterstaining. The slides were promptly examined under a fluorescence microscope (Olympus BX-51-FL; Olympus, Tokyo, Japan) equipped with epifluorescence filters and a photometric CCD camera (Sensicam; PCO Company, Kelheim, Germany). The images captured were digitized and stored in the image analysis program (MetaMorph; Molecular Devices, Palo Alto, CA). The average ratio of the TNK2 or AURKA signal number to the control probe signal number was calculated for each cancer. If the ratio of a cancer was >2.2, the cancer was defined as *TNK2* or *AURKA* amplification-positive.

Immunohistochemical Analysis

TMA sections were used for immunohistochemical staining using a Histofine Simple Stain MAX PO kit (Nichirei, Tokyo, Japan), as described previously [17]. An anti-phospho-TNK2 (Tyr284) (Millipore, Billerica, MA) was used as a primary antibody. Immunohistochemical signals were scored into three grades according to the intensity of staining: 0, 1+, and 2+. The percentages of positive cells were also scored into four categories: 0 (0%), 1+ (1–33%), 2+ (34–66%), and 3+ (67–100%). The products of the intensity and the percentage scores were used as a staining score.

Expression Plasmids

The pXJ-HA-ACK1 expression vector [7] and the FLAG-ACK1 expression vector [18] were kind gifts from Dr. Edward Manser (A-Star Neuroscience Research Partnership, Singapore) and Dr. W. Todd Miller (Stony Brook University, USA), respectively. The human *TNK2* cDNA was amplified using a polymerase chain reaction (PCR) with *PfuUltra* Hotstart DNA polymerase (Stratagene, La Jolla, CA) and the pXJ-HA-ACK1 expression vector [7] as a template; the amplified sequence was then inserted into a piggyBac cumate switch inducible vector (System Biosciences, Mountain View, CA) at the *Nhe*I and *Not*I restriction enzyme sites. The vector sequence was confirmed using DNA sequencing with a BigDye Terminator Cycle Sequencing Reaction Kit (Applied Biosystems, Tokyo, Japan) and an ABI 3100 Genetic Analyzer (Applied Biosystems).

Establishment of Stable Inducible Cell Lines

AGS cells were transfected with the piggyBac cumate switch inducible vector for TNK2 expression together with the piggyBac transposase vector (System Biosciences). To establish stable inducible cell lines, positively transposed cells were selected using puromycin (1.1 μg/ml). Since the inducible piggyBac vector features a tight cumate switch combined with an EF1-CymR repressor-T2A-Puro cassette to establish stable cell lines, the addition of cumate solution (System Biosciences) to the puromycin-selected cells leads to the induction of TNK2 expression.

Western Blot Analysis

A Western blot analysis using an anti-TNK2 polyclonal antibody (Sigma–Aldrich, St. Louis, MO) or an anti-β-tubulin monoclonal antibody (clone 2-28-33; Sigma-Aldrich) was performed as described previously [19].

Indirect Immunofluorescence Analysis

Cells were fixed with 4% paraformaldehyde, blocked with 10% normal goat serum, and probed with rabbit anti-TNK2 polyclonal antibody (Sigma–Aldrich), mouse anti-HA monoclonal antibody (16B12; Covance, Berkeley, CA), or mouse anti-FLAG monoclonal antibody (M2; Sigma–Aldrich). Indirect immunofluorescence labeling was performed by exposure to an Alexa Fluor 546 or 594-conjugated secondary antibody (Molecular Probes, Eugene, OR), and the nuclei were stained with 4′,6-diamidino-2-phenylindole (DAPI) (Sigma–Aldrich) [17]. Fluorescence signals were detected and stored as described in the "FISH analysis" section.

Transwell Migration Assay

The migration assay was performed using a six-well plate with an 8.0-μm pore polycarbonate membrane insert (Coring, Lowell, MA). The cells were seeded in the top chamber of the plate containing the transwell insert and were allowed to migrate for 24 hr at 37°C. Afterwards, the number of cells that had migrated to the bottom compartment was counted using a hemocytometer.

Non-Anchored Growth Assay

Cells were seeded in a 24-well ultra low attachment plate (Corning) and the plate was incubated at 37°C for 4 days. The number of cells growing in the media was counted using a hemocytometer.

Microarray Analysis and Mappfinder Analysis

Human gene expression was examined using the GeneChip Human Gene 1.0 ST array (Affymetrix, Santa Clara, CA). The Human Gene 1.0 ST array is comprised of 764,885 unique 25-mer oligonucleotide probes, constituting 28,869 gene probe sets. The total RNA was extracted using

an RNeasy Plus Mini Kit (Qiagen, Valencia, CA), and the quality of the total RNA was checked using an Agilent 2100 bioanalyzer and an Agilent RNA 6000 Nano kit (Agilent Technologies, Palo Alto, CA). cDNA production, antisense cRNA generation and purification, 2nd-cycle cDNA synthesis and purification, fragmentation and labeling of the cDNA, and hybridization to the GeneChip array were performed according to the manufacturer's protocol (Affymetrix). The GeneChips were finally washed and stained using the GeneChip Fluidics Station 450 (Affymetrix) and then scanned with the GeneChip Scanner 3000 7G (Affymetrix). Raw data CEL files were normalized using the Robust Multi-Array (RMA-16) algorithm in GeneSpring GX 12.5 (Agilent Technologies).

To characterize the biological processes affected in this study, we used GenMAPP (Gene Map Annotator and Pathway Profiler) version 2.1 and MAPPFinder version 2.0 [20] to produce lists of significantly regulated pathways. The MAPPFinder program can calculate the Z score (standardized difference score) and the *P*-value. A pathway was defined as having been significantly affected if the *P*-value was <0.05.

Statistical Analysis

The statistical analyses were performed using an unpaired *t*-test or chi-square test. Overall survival curves were constructed using the Kaplan–Meier method, and differences in the curves were evaluated using the log-rank test. The hazard ratio (HR) was calculated using the Cox proportional hazard model for both the univariate and multivariate analyses. JMP version 9 software (SAS Institute, Cary, NC) was used for all the statistical analyses. *P*-values <0.05 were considered statistically significant.

RESULTS

Kaplan–Meier Survival Analysis in Primary GC Patients

We previously examined the amplification status of 10 kinase genes (*PIK3CA*, *EPHB3*, *TNK2*, *PTK7*, *EGFR*, *MET*, *ERBB2*, *HCK*, *SRC*, and *AURKA*) using FISH analysis in primary GC specimens collected at the Toyohashi Municipal Hospital (Japan). To explore whether the amplifications of these genes are capable of predicting the prognosis of patients with GC, we performed a Kaplan–Meier survival analysis for a total of 271 primary GCs arising from patients for whom information on overall survival was available (Fig. 1). The results showed that the prognosis of patients with GC exhibiting *TNK2* amplification was significantly poorer than that of patients with GC without *TNK2* amplification ($P=0.0002$). They also showed that the prognosis of patients with GC exhibiting *AURKA* amplification was significantly poorer than the prognosis of patients with GC without *AURKA* amplification ($P=0.0131$). The amplification status of the other eight genes did not affect the prognosis of the GC patients.

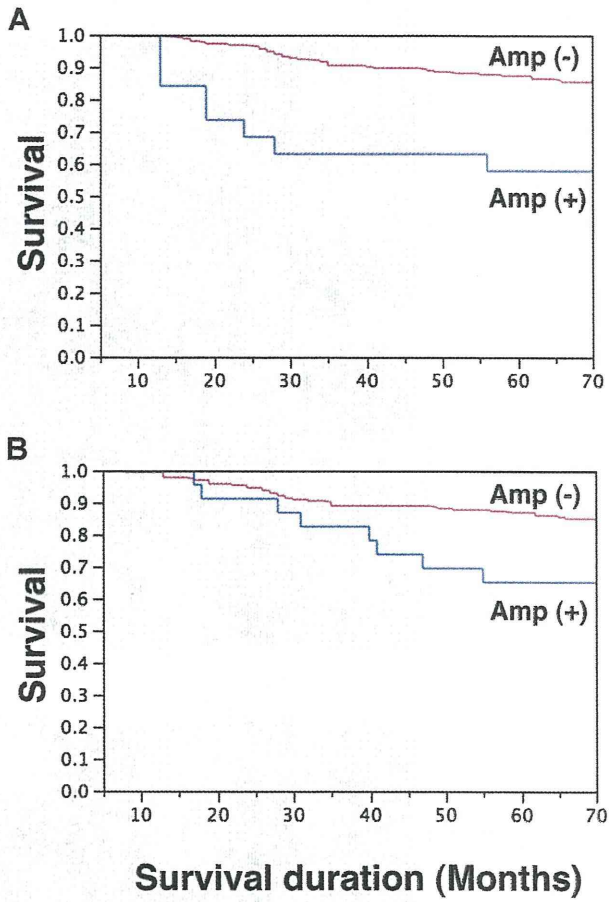

Fig. 1. Impact of *TNK2* and *AURKA* amplifications on overall survival in primary gastric cancer (GC) patients. Survival curves for GC patients ($n=271$) were generated using the Kaplan–Meier method. **A**: Comparison between GC patients with *TNK2* amplification (+) and without *TNK2* amplification (−). Log-rank $P=0.0002$. **B**: Comparison between GC patients with *AURKA* amplification (+) and without *AURKA* amplification (−). Log-rank $P=0.0131$.

Association of *TNK2* Amplification With Clinicopathological Factors in GC Patients

In our previous study, both *TNK2* and *AURKA* amplification in GC was associated with a diffuse histopathological subtype, and *TNK2* amplification was also associated with lymph node metastasis [12]. In this study, using another cohort consisting of 335 GC patients (Hamamatsu University Hospital), we attempted to investigate whether *TNK2* and *AURKA* amplification was associated with the clinicopathological features of GC patients. *TNK2* and *AURKA* amplification was observed in 36 (10.7%) of 335 primary GCs and 14 (4.5%) of 309 GCs, respectively, using FISH analysis (Fig. 2). Although no associations were found between the clinicopathological factors of sex, age, or tumor histopathology and the *TNK2* amplification status, the frequency of advanced pT stage (pT2–pT4) and lymph node metastasis (pN1–pN3) was higher in the group of GC patients with *TNK2* amplification than in the group without *TNK2* amplification ($P=0.0437$ and $P=0.0367$, respectively) (Table I). Regarding *AURKA*, no associations were found between any clinicopathological factors and the *AURKA* amplification status (data not shown). The association between *TNK2* amplification and lymph node metastasis that has been repeatedly detected in GC suggests the importance of *TNK2* amplification on lymph node metastasis.

TNK2 Amplification Was an Independent Predictor of a Poor Survival Outcome Among GC Patients

To rule out potential prognostic factors that may have confounded the *TNK2* and *AURKA* amplification results, we conducted univariate and multivariate analyses for overall survival using the Cox proportional hazard model in 271 GCs (Toyohashi Municipal Hospital) (Table II). A diffuse histopathological subtype and *AURKA* amplification were associated with significantly increased risks in univariate analyses, although the risks were attenuated in a multivariate analysis. An

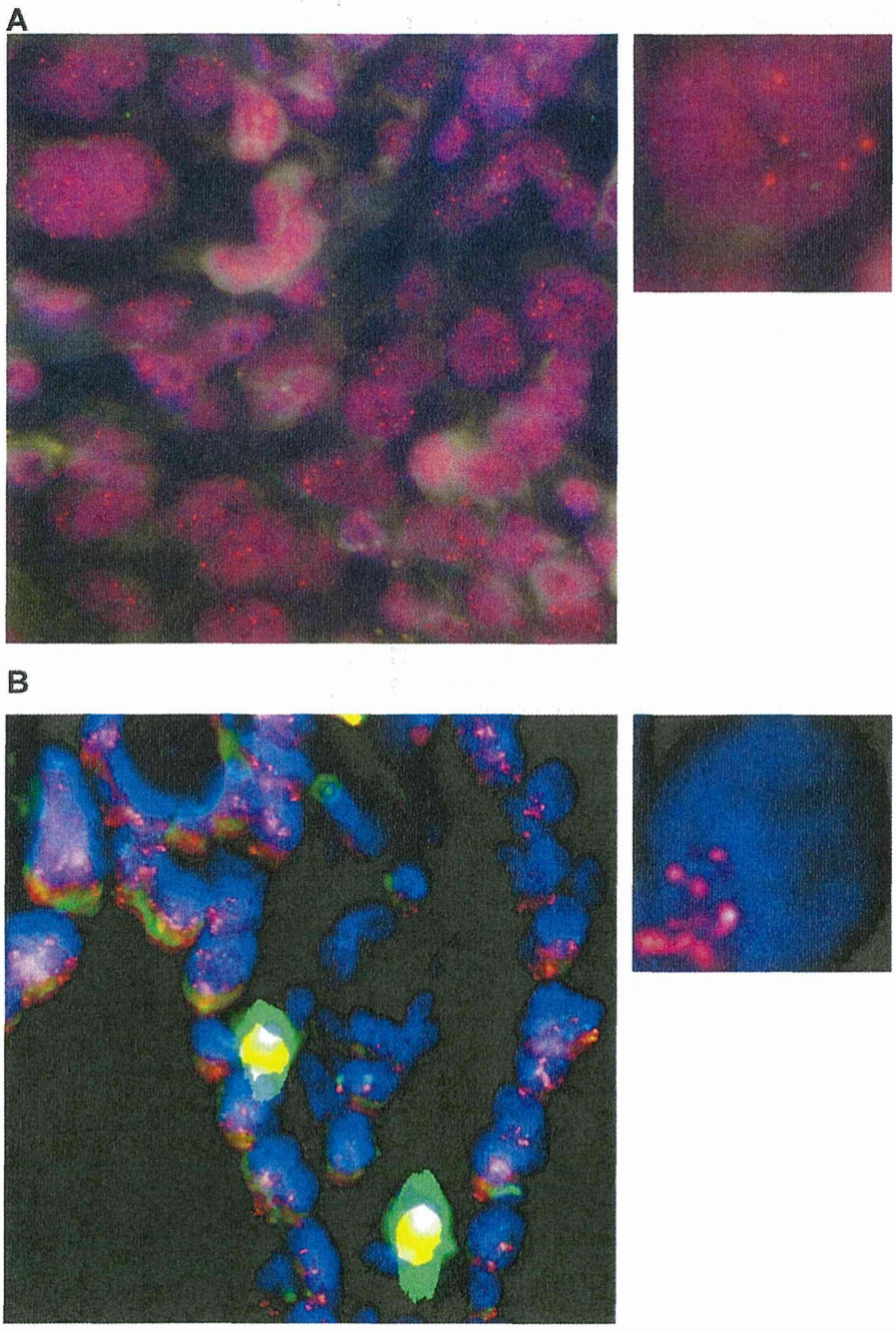

Fig. 2. *TNK2* and *AURKA* amplification in primary gastric cancer (GC). **A**: Representative result of *TNK2* amplification in GC, as shown using a FISH analysis. Right panel: higher magnification of part of the left panel. Red signals, BAC probe for the *TNK2* locus; green signals, control probe for the near centromere locus on chromosome 3. **B**: Representative result of *AURKA* amplification in GC, as shown using a FISH analysis. Right panel: a higher magnification of part of the left panel. Red signals, BAC probe for the *AURKA* locus; green signals, control probe for the near centromere locus on chromosome 20.

advanced pT stage (pT2–pT4), lymph node metastasis (pN1–pN3), and *TNK2* amplification were associated with significantly increased risks in both the univariate and multivariate analyses. The HRs of an advanced pT stage, lymph node metastasis, and *TNK2* amplification in the multivariate analyses were 1.996 [95% confidence interval (CI), 1.024–3.620; $P = 0.0425$], 3.259 (95% CI, 1.567–7.476; $P = 0.0012$), and 3.668 (95% CI, 1.513–7.968; $P = 0.0056$), respectively. These results suggested that *TNK2* amplification, as well as an advanced pT stage and lymph node metastasis, was an independent predictor of a poor survival outcome among GC patients.

TABLE I. Association Between *TNK2* Amplification and Clinicopathological Factors in 335 Patients With Primary Gastric Cancer

		TNK2		
Factor	Patient	Amplification (−) ($n=299$)	Amplification (+) ($n=36$)	*P*-value
Gender				
Male	225	202 (89.8%)	23 (10.2%)	0.6578[a]
Female	110	97 (88.2%)	13 (11.8%)	
Age				
<60	109	98 (89.9%)	11 (10.1%)	0.7882[a]
60<	226	201 (88.9%)	25 (11.1%)	
Average ± SD	63.4 ± 11.8	63.4 ± 11.8	63.0 ± 11.6	0.8473[b]
Histopathology				
Intestinal	199	173 (86.9%)	26 (13.1%)	0.0973[a]
Diffuse	136	126 (92.6%)	10 (7.4%)	
pT stage				
pT1	136	127 (93.4%)	9 (6.6%)	0.0437[a]
pT2–pT4	199	172 (86.4%)	27 (13.6%)	
pN stage				
pN0	176	163 (92.6%)	13 (7.4%)	0.0367[a]
pN1–pN3	159	136 (85.5%)	23 (14.5%)	

SD, standard deviation.
[a]Chi-square test.
[b]*t*-Test.

Relationship Between *TNK2* Amplification and pTyr284-TNK2 Expression in GC

To investigate whether *TNK2* amplification is associated with TNK2 activation, we examined the expression level of TNK2 phosphorylated at Tyr284, which was previously shown to be associated with TNK2 activation [21,22], in GCs (Toyohashi Municipal Hospital). As expected, the expression level of pTyr284-TNK2 was significantly higher in the group of GCs with *TNK2* amplification than in the group of GCs without *TNK2* amplification ($P < 0.0001$) (Fig. 3). This result indicates that *TNK2* amplification is related to the increase in activated TNK2 expression monitored by Tyr284 phosphorylation.

Effect of TNK2 Overexpression on Migration and Proliferation in Gastric Cells

To determine whether *TNK2* amplification leads to an increase in the malignant potential of gastric cells, we attempted to compare the functional effects of TNK2 in gastric cells based on their expression level. First, we established human AGS gastric cancer cells capable of

TABLE II. Cox Proportional Hazard Analysis of Potential Predictors of a Poor Prognosis in Gastric Cancer Patients (n = 271)

	Univariate analysis		Multivariate analysis	
Variable	HR [95% CI]	*P*-value	HR [95% CI]	*P*-value
Gender				
Male	1.339 [0.689–2.855]	0.4032		
Female	1			
Age				
>60	1.126 [0.620–2.121]	0.8882		
60	1			
Histopathology				
Diffuse	1.833 [1.009–3.454]	0.0467	1.662 [0.871–3.298]	0.1251
Intestinal	1		1	
pT stage				
pT2-pT4	2.899 [1.667–4.739]	0.0002	1.996 [1.024–3.620]	0.0425
pT1	1		1	
pN stage				
pN1–pN3	5.078 [2.557–11.233]	<0.0001	3.259 [1.567–7.476]	0.0012
pN0	1		1	
AURKA				
Amplification (+)	2.539 [1.098-5.174]	0.0311	2.106 [0.899–4.362]	0.0830
Amplification (−)	1		1	
TNK2				
Amplification (+)	3.887 [1.678–7.931]	0.0028	3.668 [1.513–7.968]	0.0056
Amplification (−)	1		1	

HR, hazard ratio; CI, confidence interval.

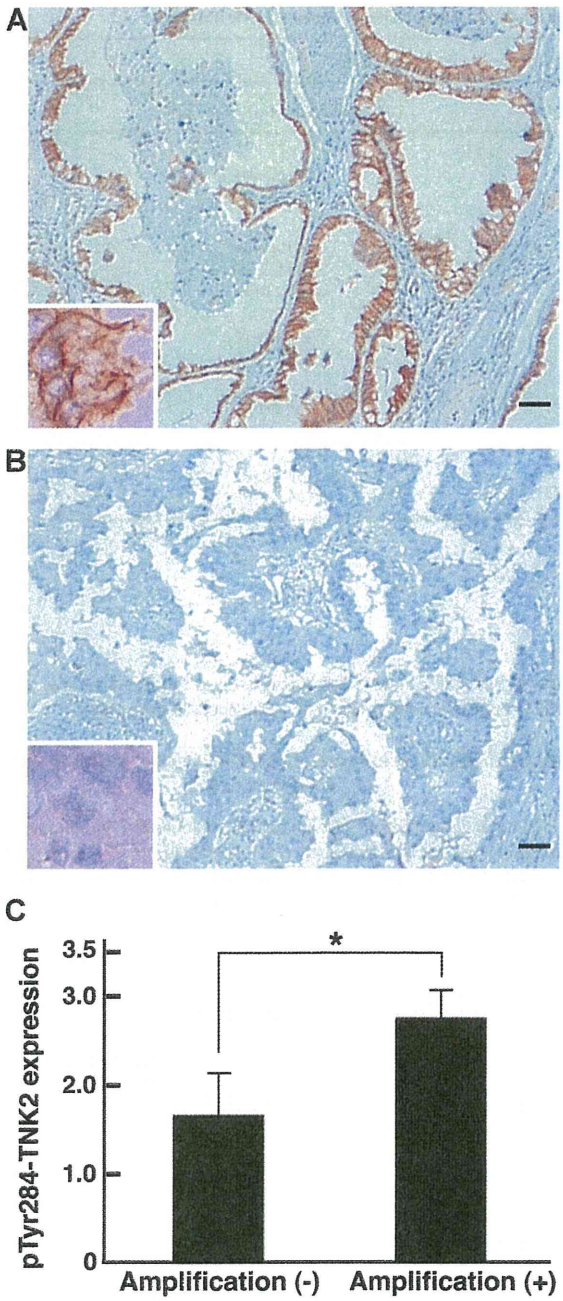

Fig. 3. Comparison of the expression levels of phosphorylated-TNK2 (Tyr284) based on *TNK2* amplification status in primary gastric cancer (GC). **A**,**B**: Representative results showing high (A) and low (B) pTyr284-TNK2 expression in GCs, as shown using an immunohistochemical analysis. The inset shows a higher magnification of part of each panel. Scale bar, 50 μm. **C**: Expression level of pTyr284-TNK2 in GC, as determined using an immunohistochemical analysis. The expression level was shown as a staining score, and the data are presented as the mean ± SE. A statistically significant difference in the pTyr284-TNK2 expression level was detected between the GC groups with *TNK2* amplification (+) and without *TNK2* amplification (−) ($P < 0.0001$).

inducibly expressing TNK2 using the piggyBac transposon vector system [23]. In detail, AGS cells were transfected with a piggyBac cumate switch inducible vector for the expression of full-length wild-type TNK2 together with the piggyBac transposase vector; positively transposed cells were then selected using puromycin. We also transfected the cells using an empty (parental) piggyBac cumate switch inducible vector and transposase vector. The expression of TNK2 protein after cumate induction was examined using a Western blot analysis using an anti-TNK2 antibody (Fig. 4A). TNK2 protein was abundantly expressed in TNK2-transposed cells after cumate induction, but not in empty vector-transposed cells.

An immunofluorescence analysis using anti-TNK2 antibody also showed abundant TNK2 protein expression in TNK2-transposed AGS cells after cumate induction. In accordance with a previous finding that TNK2 protein is localized in the cytoplasm [7], TNK2 protein was predominantly localized in the cytoplasm of the gastric cells (Fig. 4B). A predominantly cytoplasmic localization was also observed in AGS gastric cells transiently transfected with an expression vector for HA-tagged and FLAG-tagged TNK2 (Fig. 4B). These results suggest that TNK2 protein is predominantly localized in the cytoplasm of gastric cells.

The migration properties of empty vector-transposed AGS cells and TNK2-overexpressing cells were then compared using a transwell migration assay. TNK2-transposed cells showed a 2.5-fold increase in cell migration, compared with the empty vector-transposed cells (Fig. 4C). This result suggests that TNK2 overexpression endowed gastric cells with a higher migration ability.

The effect of TNK2 overexpression on the non-anchored growth of gastric cells was also compared between empty vector-transposed cells and TNK2-transposed cells. TNK2-transposed cells showed a 2.1-fold increase in cell growth, compared with the empty vector-transposed cells (Fig. 4D). This result suggests that TNK2 overexpression endowed gastric cells with an increased non-anchored growth ability.

Identification of Pathways Deregulated in AGS Gastric Cells With TNK2 Overexpression

We next considered the possibility that the alteration of global gene expression as a result of TNK2 overexpression may affect the malignant potential of gastric cells. To obtain a comprehensive view of the global gene expression profile in gastric cells with TNK2 overexpression, a microarray analysis of the mRNA transcript levels of 28,869 genes was performed using TNK2-transposed AGS cells, compared with empty vector-transposed cells. A MAPPFinder pathway analysis was then applied to the microarray data set to identify molecular pathways containing a number of altered transcript levels. Ten upregulated pathways including the TGFβ signaling pathway, the MAPK signaling pathway, the EGFR1 signaling pathway, a pathway involved in the MAPK cascade, and the p38 MAPK signaling pathway as well as two downregulated pathways involved in the G1 to S cell cycle control and hedgehog signaling were identified (Table III). These results suggest that the above-mentioned pathways are aberrantly regulated in GC cells with TNK2 overexpression.

DISCUSSION

In this study, a Kaplan–Meier analysis showed that the prognosis of patients with GC exhibiting *TNK2* or *AURKA* amplification was significantly poorer than the prognosis of patients with GC without *TNK2* or *AURKA* amplification. A further multivariate analysis revealed that *TNK2* amplification, but not *AURKA* amplification, in addition to an advanced pT stage and lymph node metastasis were independent predictors of a poor survival outcome among the GC patients. To investigate whether *TNK2* amplification leads to an increase in the malignant potential of gastric cells, we established GC cells capable of

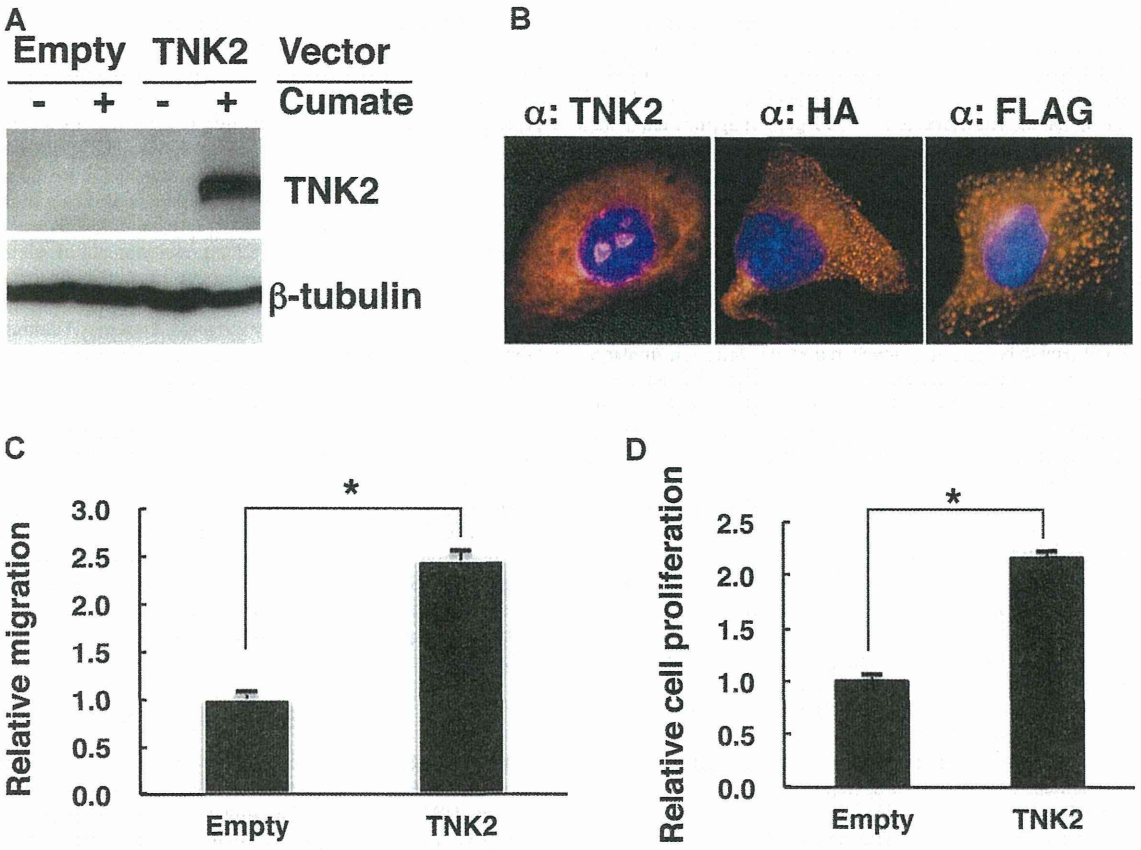

Fig. 4. Comparison of TNK2 functional effects on gastric cancer (GC) cells based on their TNK2 expression level. **A**: Establishment of AGS human GC cell lines inducibly expressing TNK2 protein. TNK2 proteins were detected in AGS stable cell lines expressing TNK2 in the presence of cumate using a Western blot analysis with an anti-TNK2 antibody. Lysates from empty vector-transposed cells and cells inducibly expressing TNK2 were analyzed. β-tubulin protein was also analyzed as an internal control. Endogenous TNK2 protein was barely detected using our detection system. **B**: Immunofluorescence detection of TNK2 proteins expressed in the GC cell lines used in (A) in the presence of cumate (left panel). TNK2 proteins in AGS cells transiently transfected with an expression vector for HA-tagged TNK2 and FLAG-tagged TNK2 were immunofluorescently detected in the middle panel and right panel, respectively. TNK2 protein, red; Nuclei, blue. **C**: Comparison of migration ability between empty vector-transposed AGS GC cells and TNK2-transposed cells using a transwell migration assay. Data are means ± SE of three independent experiment. The average of the percentage of migrated cells in empty vector-transposed cells was set to 1.0. The * symbol indicates a statistical significance ($P < 0.01$). **D**: Comparison of non-anchored growth ability between empty vector-transposed AGS GC cells and TNK2-transposed cells using a cell growth assay with an ultra low attachment plate. Data are means ± SE of three independent experiment. The average number of proliferating cells among the empty vector-transposed cells was set at 1.0. The * symbol indicates a statistical significance ($P < 0.001$).

TABLE III. Upregulated or Downregulated Pathways in the Human Gastric Cancer Cell Line AGS With the Induction of TNK2 Overexpression

MAPP pathway name	Z score	*P*-value
Upregulated		
TGFβ signaling pathway	5.135	0.001
Human insulin signalling	3.865	0.002
MAPK signaling pathway	3.845	0.004
Hypertrophy model	4.471	0.009
Myometrial relaxation and contraction pathways	3.288	0.01
EGFR1 signaling pathway	2.768	0.023
Adipogenesis human	2.642	0.031
MAPK cascade	3.329	0.037
Signaling of hepatocyte growth factor receptor	3.118	0.043
p38 MAPK signaling pathway	2.993	0.046
Downregulated		
G1 to S cell cycle control	5.791	0.001
Hedgehog signaling pathway	5.244	0.034

A positive Z score indicates that there are more genes meeting the criterion in a MAPP than would be expected by random chance.

inducibly expressing TNK2 using the piggyBac transposon vector system. TNK2-transposed GC cells showed an increase in cell migration and non-anchored cell growth, compared with empty vector-transposed GC cells. Some cancer-related pathways were also shown to be aberrantly regulated in TNK2-overexpressing GC cells using microarray and pathway analyses. These results suggested that *TNK2* gene amplification is an independent predictor of a poor prognosis among patients with GC and leads to an increase in the malignant potential of GC cells, providing a new and important link between gene amplification and GC. To the best of our knowledge, this is the first demonstration of *TNK2* amplification as a prognostic factor in human cancer.

van der Horst et al. [10] previously performed a Kaplan–Meier analysis of BALB/c mice inoculated with TNK2-overexpressing cells or control cells and showed that TNK2 overexpression enhances metastasis and mortality. Another group reported that TNK2 Tyr284 phosphorylation, which is involved in its kinase activation, was negatively correlated with the survival of human prostate and pancreatic

cancer patients [21,22]. These results suggest that TNK2 activation defines the survival of human cancer patients; however, the association between *TNK2* amplification and the survival duration of patients has not been previously reported for any human cancers. Our results clearly demonstrated, for the first time, that *TNK2* gene amplification is an independent predictor of a poor prognosis among patients with GC. We also found that an advanced pT stage and lymph node metastasis were independent predictors of a poor prognosis in patients with GC, as has been previously reported [24]; this agreement suggests that the presently performed survival analyses were valid. In the present study, an increased ability for cell migration and non-anchored cell growth, which are hallmarks of cells exhibiting a higher malignant potential, were detected in GC cells with TNK2 overexpression. A role of TNK2 in migration and growth has been previously reported in human mammary, prostatic, and renal cells and mouse cells [4,8,10,18,25–27], but not in gastric cells; thus, our results are the first demonstration of such a role in gastric cells. Based on the results of the association analysis (Table I) and the survival analysis (Table II), we suspect that an aggressive role of TNK2 in cell migration and non-anchored cell growth might be partly involved in not only progression to an advanced pT stage and lymph node metastasis, but also a poor survival outcome. Regarding events downstream of TNK2, more than 10 proteins have been reported to interact with TNK2 [1,4,7–9]; however, genome-wide expression profiling after TNK2 overexpression has not been previously performed. We detected a total of 12 deregulated pathways using microarray and pathway analyses. Among them, the upregulation of the MAPK signaling pathway and the EGFR signaling pathway have been reported to be related to neoplasia [28,29]. The TGFβ signaling pathway, which is also upregulated in gastric cells showing TNK2 overexpression, has also been reported to exert not only anti-oncogenic activities, but pro-oncogenic activities, for example, the dysregulation of the cell cycle, the promotion of the epithelial–mesenchymal transition, the induction of angiogenesis, and increases in proteases and extracellular matrix [30]. Therefore, these pathways could be involved in our finding that *TNK2* amplification is a predictor of a poor prognosis in patients with GC.

The effects of TNK2 knockdown have been reported in several papers [5,6,8,26,27,31,32]. siRNA against TNK2 decreased cell viability and apoptosis induction in Ewing's sarcoma cells [31]. Silencing of TNK2 led to diminished ruffling and migration in DU145 prostate cancer cells and COS-7 monkey kidney fibroblasts upon GAS6-Axl signaling [6]. Additionally, in LNCaP prostate cancer cells, TNK2 knockdown suppressed the phosphorylation (pTyr267) of AR, which is a downstream effector protein of TNK2 [32], and silencing experiments in A498 kidney cancer cells containing a somatic mutation (Ser985Asn) in the TNK2 ubiquitin association domain demonstrated the role of the TNK2 mutation in the enhancement of cell proliferation and migration as well as the epithelial–mesenchymal transition [27]. The TNK2 activation arising from *TNK2* amplification in a subset of GCs suggests that TNK2 knockdown suppresses various cellular phenomena, such as cell proliferation and migration, in GC cells with *TNK2* amplification.

In the present study, *AURKA* amplification was statistically associated with a decreased overall survival among patients with GC. Although AURKA overexpression has been reportedly associated with a poor survival outcome in patients with bladder cancer, hepatocellular carcinoma, head and neck squamous cell carcinoma, endometrioid ovarian cancer, and a subset of breast cancer [33–37], the present report is the first to find that *AURKA* amplification is a predictor of a poor prognosis among patients with GC. Since the function of AURKA is mainly related to centrosome function and spindle assembly and the overexpression of AURKA results in a defective spindle assembly checkpoint, allowing abnormal chromosomal separation and leading to aneuploidy and the induction of chromosome instability [38], such a phenomenon in gastric cells is thought to lead to the poor survival outcome of GC patients.

In this article, we successfully established cumate-inducible stable GC cell lines utilizing the piggyBac transposon vector system. Transposon technology is an attractive non-viral gene delivery model that allows for efficient genomic integration in a variety of cell types [39]. Among the several transposon systems that are available, the piggyBac transposon, which was isolated from the *Trichoplusia ni* genome, has been optimized for gene transfer into mammalian cells [39,40]. In practice, the TNK2 expression status in our cell lines after puromycin selection in the presence of cumate clearly demonstrated an abundance of TNK2 expression in almost all the cells.

Prognostic markers may play another clinical role in the treatment of cancer patients by leading to the identification of patient subgroups that are suited for current molecularly targeted therapy. Antibodies and inhibitors targeting specific molecules are actively being developed worldwide, and some of these agents have been demonstrated to be effective in malignant neoplasias, such as leukemia, breast carcinoma, and non-small cell lung carcinoma [41–43]. Regarding TNK2, small molecule inhibitors of TNK2 have been recently developed [21,22,44]. For example, AIM-100, which is the first and best-studied TNK2 inhibitor, has been shown to suppress pTyr284-TNK2 expression and cell growth [21,22]. Moreover, this inhibitor suppressed the phosphorylation (pTyr267) of AR, pTyr267-AR recruitment to androgen-regulated gene regulatory sequences, and pTyr267-AR transcriptional activity [21]. Therefore, GC patients with *TNK2* amplification might benefit clinically from TNK2 inhibitors in the future.

ACKNOWLEDGMENTS

We are grateful to Dr. Edward Manser (A-Star Neuroscience Research Partnership, Singapore) and Dr. W. Todd Miller (Stony Brook University, USA) for providing us with the Ack1 expression vector. We would like to acknowledge Ms. K. Maruyama (Hamamatsu University School of Medicine) for her technical assistance. This work was supported in part by a Grant-in-Aid from the Ministry of Health, Labour and Welfare (21-1), a Grant-in-Aid from the Japan Society for the Promotion of Science (25460476), and a Grant-in-Aid from the Ministry of Education, Culture, Sports, Science and Technology (221S0001).

REFERENCES

1. Manser E, Leung T, Salihuddin H, et al.: A non-receptor tyrosine kinase that inhibits the GTPase activity of p21cdc42. Nature 1993;363:364–367.
2. Mahajan K, Mahajan NP: Shepherding AKT and androgen receptor by Ack1 tyrosine kinase. J Cell Physiol 2010;224:327–333.
3. Galisteo ML, Yang Y, Ureña J, et al.: Activation of the nonreceptor protein tyrosine kinase Ack by multiple extracellular stimuli. Proc Natl Acad Sci USA 2006;103:9796–9801.
4. Mahajan NP, Whang YE, Mohler JL, et al.: Activated tyrosine kinase Ack1 promotes prostate tumorigenesis: Role of Ack1 in polyubiquitination of tumor suppressor Wwox. Cancer Res 2005; 65:10514–10523.
5. Shen F, Lin Q, Gu Y, et al.: Activated Cdc42-associated kinase 1 is a component of EGF receptor signaling complex and regulates EGF receptor degradation. Mol Biol Cell 2007;18:732–742.
6. Pao-Chun L, Chan PM, Chan W, et al.: Cytoplasmic ACK1 interaction with multiple receptor tyrosine kinases is mediated by Grb2: An analysis of ACK1 effects on Axl signaling. J Biol Chem 2009;284:34954–34963.
7. Teo M, Tan L, Lim L, et al.: The tyrosine kinase ACK1 associates with clathrin-coated vesicles through a binding motif shared by arrestin and other adaptors. J Biol Chem 2001;276:18392–18398.
8. Mahajan NP, Liu Y, Majumder S, et al.: Activated Cdc42-associated kinase Ack1 promotes prostate cancer progression via androgen receptor tyrosine phosphorylation. Proc Natl Acad Sci USA 2007;104:8438–8443.

9. Mahajan K, Coppola D, Challa S, et al.: Ack1 mediated AKT/PKB tyrosine 176 phosphorylation regulates its activation. PLoS ONE 2010;5:e9646.
10. van der Horst EH, Degenhardt YY, Strelow A, et al.: Metastatic properties and genomic amplification of the tyrosine kinase gene ACK1. Proc Natl Acad Sci USA 2005;102:15901–15906.
11. Sugimura H, Mori H, Nagura K, et al.: Fluorescence in situ hybridization analysis with a tissue microarray: 'FISH and chips' analysis of pathology archives. Pathol Int 2010;60:543–550.
12. Kiyose S, Nagura K, Tao H, et al.: Detection of kinase amplifications in gastric cancer archives using fluorescence in situ hybridization. Pathol Int 2012;62:477–484.
13. Jehan Z, Bavi P, Sultana M, et al.: Frequent PIK3CA gene amplification and its clinical significance in colorectal cancer. J Pathol 2009;219:337–346.
14. Jørgensen JT, Hersom M: HER2 as a prognostic marker in gastric cancer—a systematic analysis of data from the literature. J Cancer 2012;3:137–144.
15. Grillo F, Fassan M, Ceccaroli C, et al.: The reliability of endoscopic biopsies in assessing HER2 status in gastric and gastroesophageal junction cancer: A study comparing biopsies with surgical samples. Transl Oncol 2013;6:10–16.
16. Kim HR, Kim DJ, Kang DR, et al.: Fibroblast growth factor receptor 1 gene amplification is associated with poor survival and cigarette smoking dosage in patients with resected squamous cell lung cancer. J Clin Oncol 2013;31:731–737.
17. Shinmura K, Goto M, Suzuki M, et al.: Reduced expression of MUTYH with suppressive activity against mutations caused by 8-hydroxyguanine is a novel predictor of a poor prognosis in human gastric cancer. J Pathol 2011;225:414–423.
18. Prieto-Echagüe V, Gucwa A, Brown DA, et al.: Regulation of Ack1 localization and activity by the amino-terminal SAM domain. BMC Biochem 2010;11:42.
19. Shinmura K, Bennett RA, Tarapore P, et al.: Direct evidence for the role of centrosomally localized p53 in the regulation of centrosome duplication. Oncogene 2007;26:2939–2944.
20. Dahlquist KD, Salomonis N, Vranizan K, et al.: GenMAPP, a new tool for viewing and analyzing microarray data on biological pathways. Nat Genet 2002;31:19–20.
21. Mahajan K, Challa S, Coppola D, et al.: Effect of Ack1 tyrosine kinase inhibitor on ligand-independent androgen receptor activity. Prostate 2010;70:1274–1285.
22. Mahajan K, Coppola D, Chen YA, et al.: Ack1 tyrosine kinase activation correlates with pancreatic cancer progression. Am J Pathol 2012;180:1386–1393.
23. Ding S, Wu X, Li G, et al.: Efficient transposition of the piggyBac (PB) transposon in mammalian cells and mice. Cell 2005;122:473–483.
24. Qiu MZ, Cai MY, Zhang DS, et al.: Clinicopathological characteristics and prognostic analysis of Lauren classification in gastric adenocarcinoma in China. J Transl Med 2013;11:58.
25. Howlin J, Rosenkvist J, Andersson T: TNK2 preserves epidermal growth factor receptor expression on the cell surface and enhances migration and invasion of human breast cancer cells. Breast Cancer Res 2008;10:R36.
26. Liu Z, Adams HC III, Whitehead IP: The rho-specific guanine nucleotide exchange factor Dbs regulates breast cancer cell migration. J Biol Chem 2009;284:15771–15780.
27. Chua BT, Lim SJ, Tham SC, et al.: Somatic mutation in the ACK1 ubiquitin association domain enhances oncogenic signaling through EGFR regulation in renal cancer derived cells. Mol Oncol 2010; 4:323–334.
28. Santarpia L, Lippman SM, El-Naggar AK: Targeting the MAPK-RAS-RAF signaling pathway in cancer therapy. Expert Opin Ther Targets 2012;16:103–119.
29. Lee J, Kim S, Kim P, et al.: A novel proteomics-based clinical diagnostics technology identifies heterogeneity in activated signaling pathways in gastric cancers. PLoS ONE 2013;8:e54644.
30. Achyut BR, Yang L: Transforming growth factor-β in the gastrointestinal and hepatic tumor microenvironment. Gastroenterology 2011;141:1167–1178.
31. Arora S, Gonzales IM, Hagelstrom RT, et al.: RNAi phenotype profiling of kinases identifies potential therapeutic targets in Ewing's sarcoma. Mol Cancer 2010;9:218.
32. Liu Y, Karaca M, Zhang Z, et al.: Dasatinib inhibits site-specific tyrosine phosphorylation of androgen receptor by Ack1 and Src kinases. Oncogene 2010;29:3208–3216.
33. Sen S, Zhou H, Zhang RD, et al.: Amplification/overexpression of a mitotic kinase gene in human bladder cancer. J Natl Cancer Inst 2002;94:1320–1329.
34. Jeng YM, Peng SY, Lin CY, et al.: Overexpression and amplification of Aurora-A in hepatocellular carcinoma. Clin Cancer Res 2004;10:2065–2071.
35. Reiter R, Gais P, Jütting U, et al.: Aurora kinase A messenger RNA overexpression is correlated with tumor progression and shortened survival in head and neck squamous cell carcinoma. Clin Cancer Res 2006;12:5136–5141.
36. Yang F, Guo X, Yang G, et al.: AURKA and BRCA2 expression highly correlate with prognosis of endometrioid ovarian carcinoma. Mod Pathol 2011;24:836–845.
37. Siggelkow W, Boehm D, Gebhard S, et al.: Expression of aurora kinase A is associated with metastasis-free survival in node-negative breast cancer patients. BMC Cancer 2012;12: 562.
38. Lens SM, Voest EE, Medema RH: Shared and separate functions of polo-like kinases and aurora kinases in cancer. Nat Rev Cancer 2010;10:825–841.
39. Macdonald J, Taylor L, Sherman A, et al.: Efficient genetic modification and germ-line transmission of primordial germ cells using piggyBac and Tol2 transposons. Proc Natl Acad Sci USA 2012;109:E1466–E1472.
40. Cary LC, Goebel M, Corsaro BG, et al.: Transposon mutagenesis of baculoviruses: Analysis of Trichoplusia ni transposon IFP2 insertions within the FP-locus of nuclear polyhedrosis viruses. Virology 1989;172:156–169.
41. Breccia M, Salaroli A, Molica M, et al.: Systematic review of dasatinib in chronic myeloid leukemia. Onco Targets Ther 2013;6:257–265.
42. Yonemori K, Tsuta K, Shimizu C, et al.: Immunohistochemical expression of HER1, HER3, and HER4 in HER2-positive breast cancer patients treated with trastuzumab-containing neoadjuvant chemotherapy. J Surg Oncol 2010;101:222–227.
43. Lee CK, Brown C, Gralla RJ, et al.: Impact of EGFR inhibitor in non-small cell lung cancer on progression-free and overall survival: A meta-analysis. J Natl Cancer Inst 2013;105: 595–605.
44. Jiao X, Kopecky DJ, Liu J, et al.: Synthesis and optimization of substituted furo[2,3-d]-pyrimidin-4-amines and 7H-pyrrolo[2,3-d] pyrimidin-4-amines as ACK1 inhibitors. Bioorg Med Chem Lett 2012;22:6212–6217.

World Journal of Gastroenterology

Online Submissions: http://www.wjgnet.com/esps/
wjg@wjgnet.com
doi:10.3748/wjg.v18.i47.6935

World J Gastroenterol 2012 December 21; 18(47): 6935-6942
ISSN 1007-9327 (print) ISSN 2219-2840 (online)

ORIGINAL ARTICLE

Impaired suppressive activities of human MUTYH variant proteins against oxidative mutagenesis

Kazuya Shinmura, Masanori Goto, Hong Tao, Shun Matsuura, Tomonari Matsuda, Haruhiko Sugimura

Kazuya Shinmura, Masanori Goto, Hong Tao, Shun Matsuura, Haruhiko Sugimura, Department of Tumor Pathology, Hamamatsu University School of Medicine, Shizuoka 431-3192, Japan
Tomonari Matsuda, Research Center for Environmental Quality Management, Kyoto University, Shiga 520-0811, Japan
Author contributions: Shinmura K conceived the study, performed the experiments, and wrote the manuscript; Goto M, Tao H and Matsuura S performed part of the experiments; Matsuda T and Sugimura H analyzed the data; all the authors were involved in the writing of the paper and approved the final version of the manuscript.
Supported by Grants from the Ministry of Health, Labour and Welfare (21-1); the Japan Society for the Promotion of Science (22590356 and 22790378); the Hamamatsu Foundation for Science and Technology Promotion, the Ministry of Education, Culture, Sports, Science and Technology (221S0001); the Takeda Science Foundation; the Aichi Cancer Research Foundation; and the Smoking Research Foundation
Correspondence to: Kazuya Shinmura, MD, PhD, Department of Tumor Pathology, Hamamatsu University School of Medicine, 1-20-1 Handayama, Higashi Ward, Hamamatsu, Shizuoka 431-3192, Japan. kzshinmu@hama-med.ac.jp
Telephone: +81-53-4352220 Fax: +81-53-4352225
Received: June 20, 2012 Revised: September 19, 2012
Accepted: September 22, 2012
Published online: December 21, 2012

Abstract

AIM: To investigate the suppressive activity of MUTYH variant proteins against mutations caused by oxidative lesion, 8-hydroxyguanine (8OHG), in human cells.

METHODS: p.R154H, p.M255V, p.L360P, and p.P377L MUTYH variants, which were previously found in patients with colorectal polyposis and cancer, were selected for use in this study. Human H1299 cancer cell lines inducibly expressing wild-type (WT) MUTYH (type 2) or one of the 4 above-mentioned MUTYH variants were established using the piggyBac transposon vector system, enabling the genomic integration of the transposon sequence for MUTYH expression. MUTYH expression was examined after cumate induction using Western blotting analysis and immunofluorescence analysis. The intracellular localization of MUTYH variants tagged with FLAG was also immunofluorescently examined. Next, the mutation frequency in the *supF* of the shuttle plasmid pMY189 containing a single 8OHG residue at position 159 of the *supF* was compared between empty vector cells and cells expressing WT MUTYH or one of the 4 MUTYH variants using a *supF* forward mutation assay.

RESULTS: The successful establishment of human cell lines inducibly expressing WT MUTYH or one of the 4 MUTYH variants was concluded based on the detection of MUTYH expression in these cell lines after treatment with cumate. All of the MUTYH variants and WT MUTYH were localized in the nucleus, and nuclear localization was also observed for FLAG-tagged MUTYH. The mutation frequency of *supF* was 2.2×10^{-2} in the 8OHG-containing pMY189 plasmid and 2.5×10^{-4} in WT pMY189 in empty vector cells, which was an 86-fold increase with the introduction of 8OHG. The mutation frequency (4.7×10^{-3}) of *supF* in the 8OHG-containing pMY189 plasmid in cells overexpressing WT MUTYH was significantly lower than in the empty vector cells ($P < 0.01$). However, the mutation frequencies of the *supF* in the 8OHG-containing pMY189 plasmid in cells overexpressing the p.R154H, p.M255V, p.L360P, or p.P377L MUTYH variant were 1.84×10^{-2}, 1.55×10^{-2}, 1.91×10^{-2}, and 1.96×10^{-2}, respectively, meaning that no significant difference was observed in the mutation frequency between the empty vector cells and cells overexpressing MUTYH mutants.

CONCLUSION: The suppressive activities of p.R154H, p.M255V, p.L360P, and p.P377L MUTYH variants against mutations caused by 8OHG are thought to be severely impaired in human cells.

Key words: 8-hydroxyguanine; Mutation; MUTYH; MUTYH-associated polyposis; Oxidative mutagenesis; *supF* forward mutation assay; piggyBac transposon; Colorectal polyposis

Peer reviewers: Dr. Anthony T Yeung, BS, MS, PhD, Fox Chase Cancer Center, Room R404, 333 Cottman Avenue, Philadelphia, PA 19111-2497, United States; Yeun-Jun Chung, MD, PhD, Professor, Director, Department of Microbiology, Integrated Research Center for Genome Polymorphism, the Catholic University Medical College, 505 Banpo-dong, Socho-gu, Seoul 137-701, South Korea

Shinmura K, Goto M, Tao H, Matsuura S, Matsuda T, Sugimura H. Impaired suppressive activities of human MUTYH variant proteins against oxidative mutagenesis. *World J Gastroenterol* 2012; 18(47): 6935-6942 Available from: URL: http://www.wjgnet.com/1007-9327/full/v18/i47/6935.htm DOI: http://dx.doi.org/10.3748/wjg.v18.i47.6935

INTRODUCTION

8-hydroxyguanine (8OHG) is an oxidatively damaged form of guanine[1], and because 8OHG can pair with adenine as well as cytosine, the formation of 8OHG in DNA causes a G:C to T:A transversion mutation[2]. To prevent such mutations, excision repair proteins, such as MUTYH (OMIM 604933), that act on 8OHG are present in human cells. The MUTYH protein is a DNA glycosylase that catalyzes the removal of adenine that is mispaired with 8OHG in double-stranded DNA[3-7]. Two major MUTYH proteins, type 1 and type 2, are expressed in human cells as a result of multiple transcription initiation sites and the alternative splicing of mRNA transcripts[4,7]. Because the type 1 protein contains a mitochondrial targeting signal (MTS) in its N-terminal, it is localized in the mitochondria. In contrast, the type 2 protein lacks the N-terminal 14 amino acids of type 1, and this absence leads to the destruction of the MTS; consequently, the type 2 protein is localized in the nucleus[4,7].

Biallelic germline mutations in the *MUTYH* gene are responsible for MUTYH-associated polyposis (MAP) (OMIM 608456), which is a hereditary disease characterized by multiple colorectal adenomas and carcinomas[8-12]. Most biallelic *MUTYH* carriers have between 10 and a few hundred colorectal polyps, meaning that MAP shows a phenotypic overlap with two other hereditary colorectal polyposis syndromes: familial adenomatous polyposis (FAP: OMIM 175100) and attenuated FAP (AFAP: OMIM 175100), both of which are caused by inactivation of the *APC* gene (OMIM 611731)[13,14]. Therefore, screening for germline mutations in *MUTYH* and *APC* is important in candidate patients with multiple colorectal polyps. However, even when *MUTYH* gene variations are detected in the mutation screening, if information regarding the level of the repair activities of the MUTYH variants is lacking, a correct diagnosis of MAP is impossible to make. Thus far, 300 unique DNA variants of the *MUTYH* gene have been reported in the Leiden Open Variation Database (http://www.lovd.nl/2.0/index_list.php)[15], and the proportion of missense *MUTYH* variations in the database is larger than nonsense mutations or truncating mutations. For most of the genes, a functional analysis is needed to determine whether the activity of a protein encoded by a missense variant is severely reduced. Thus, the effect of *MUTYH* variations on repair activity should be examined; however, so far, only a small number of *MUTYH* variations has been investigated[16-27]. In most of these studies, the DNA glycosylase activities of the variant recombinant proteins were analyzed using a DNA cleavage assay to test the abilities of the variants to cleave double-stranded oligonucleotides containing an A:8OHG mispair *in vitro*[18,19,21,23-27]. However, because examining the repair activity of MUTYH variant proteins from multiple aspects would lead to a more definitive judgment of the pathogenicity of MUTYH variants and MUTYH has the ability to regulate the mutation frequency in human cells *in vivo*[28-30], evaluating the mutation frequency in human cells is also valuable. However, at present, the activities of MUTYH variants in the regulation of mutation suppression in human cells *in vivo* have not been previously reported. Therefore, in this paper, we evaluated the suppressive activities of MUTYH variant proteins against oxidative mutagenesis in human cells. We recently determined the DNA glycosylase activities of 14 type 2 (nuclear form) MUTYH variants using a DNA cleavage assay[27], and based on those results, p.R154H, p.M255V, p.L360P, and p.P377L type 2 proteins were chosen from the tested variants, and their abilities to suppress mutations caused by 8OHG in human cells were analyzed in this study. As far as we know, this is the first report to analyze the suppressive activities of MUTYH variants against oxidative mutagenesis in human cells.

The Human Genome Variation Society (http://www.hgvs.org/) recommends using the transcript variant α5 (NM_001128425.1), which encodes the longest isoform (549 amino acids), as a reference sequence. Therefore, the type 2 proteins p.R154H, p.M255V, p.L360P, and p.P377L used in this study correspond to the reference proteins p.R182H, p.M283V, p.L388P, and p.P405L, respectively.

MATERIALS AND METHODS

Cell line

The human cancer cell line H1299 was obtained from the American Type Culture Collection (Manassas, VA). Cells were maintained at 37 ℃ in RPMI1640 medium supplemented with 10% fetal bovine serum and penicillin/streptomycin under a 5% CO_2 atmosphere. The study design was approved by an institutional review board.

Construction of expression plasmid

Human wild-type (WT) and variant (p.R154H, p.M255V, p.L360P, and p.P377L) MUTYH type 2 cDNAs were polymerase chain reaction-amplified with *PfuUltr*a Hot-

start DNA polymerase (Stratagene, La Jolla, CA) and the MUTYH-type 2/pET25b(+) expression vector[27] as a template; the amplified sequence was then inserted into a piggyBac cumate switch inducible vector (System Biosciences, Mountain View, CA) at the *Nhe*I and *Not*I restriction enzyme sites. A WT MUTYH type 2 expression vector with a C-terminal FLAG tag was previously constructed using the pcDNA3.1 expression vector (Invitrogen, Carlsbad, CA)[31]; in this study, the variants were generated using site-directed mutagenesis with a QuikChange Site-directed Mutagenesis kit (Stratagene). All of the vectors were confirmed using DNA sequencing with a BigDye Terminator Cycle Sequencing Reaction Kit (Applied Biosystems, Tokyo, Japan) and an ABI 3100 Genetic Analyzer (Applied Biosystems).

Transfection

A plasmid vector was transfected into H1299 cells using Lipofectamine 2000 reagent (Invitrogen) according to the supplier's recommendations.

Establishment of stable inducible cell lines

H1299 cells were transfected with the cumate switch inducible vector for MUTYH expression together with the piggyBac transposase vector (System Biosciences). To establish stable inducible cell lines, positively transposed cells were selected using puromycin (1 μg/mL). Because the inducible piggyBac vector features a tight cumate switch combined with the EF1-CymR repressor-T2A-Puro cassette to establish stable cell lines, the addition of cumate solution (System Biosciences) to the puromycin-selected cells led to the induction of MUTYH expression.

Western blotting analysis

Cells were harvested in lysis buffer containing 50 mmol/L HEPES (pH 7.5), 150 mmol/L NaCl, 0.1% sodium dodecyl sulfate (SDS), 1.0% Triton X-100, 0.5% sodium deoxycholate, 100 mmol/L sodium fluoride, 1 mmol/L sodium orthovanadate, and a protease inhibitor cocktail (Sigma-Aldrich, St. Louis, MO), and the whole-cell extracts were mixed with an equal volume of 2 × SDS sample buffer and boiled. The extract was then subjected to SDS-polyacrylamide gel electrophoresis, and the proteins obtained were electrophoretically transferred to a polyvinylidene fluoride membrane (GE Healthcare Bio-Science, Piscataway, NJ). The membrane was blocked with nonfat milk at room temperature (RT) for 1 h and incubated with an anti-MUTYH monoclonal antibody (clone 4D10; Abnova, Taipei, Taiwan) or an anti-β-tubulin monoclonal antibody (clone 2-28-33; Sigma-Aldrich) at RT for 1 h. After washing with PBS containing 0.05% Tween-20 (PBS-T), the membrane was incubated with an anti-mouse HRP-conjugated secondary antibody (GE Healthcare Bio-Science) at RT for 1 h. The membrane was then washed with PBS-T, and immunoreactivity was visualized using an ECL chemiluminescence system (GE Healthcare Bio-Science).

Indirect immunofluorescence analysis

Cells were fixed with 10% formalin at RT or 4% paraformaldehyde at 4 ℃. The cells were permeabilized with 1% Nonidet P-40 in PBS for 5 min and incubated with 10% normal goat serum blocking solution (DAKO, Kyoto, Japan) for 30 min. The cells were then probed with mouse anti-MUTYH monoclonal antibody (4D10) or mouse anti-FLAG M2 monoclonal antibody (Sigma-Aldrich) at RT for 1 h. Indirect immunofluorescence labeling was performed by incubation with an Alexa Fluor 594-conjugated secondary antibody (Molecular Probes, Eugene, OR) at RT for 1 h, and the nuclei were stained with 4',6-diamidino-2-phenylindole (DAPI) (Sigma-Aldrich). The immunostained cells were examined under a fluorescence microscope (Olympus BX-51-FL; Olympus, Tokyo, Japan) equipped with epifluorescence filters and a photometric CCD camera (Sensicam; PCO Company, Kelheim, Germany). The captured images were digitized and stored using an image analysis program (MetaMorph; Molecular Devices, Palo Alto, CA).

Shuttle vector plasmid and an indicator bacterial strain

The plasmid pMY189 and the indicator *Escherichia coli* (*E. coli*) strain KS40/pKY241 were used for the *supF* forward mutation assay, as reported previously[30,32]. pMY189 is a shuttle vector containing the bacterial suppressor tRNA (*supF*) gene. KS40 is a nalidixic acid-resistant (*gyrA*) derivative of MBM7070 with genotype *lacZ* (*am*), *CA7070*, *lacY1*, *hsdR*, *hsdM*, Δ(*araABC-leu*)7679, *galU*, *galK*, *rpsL*, *thi*. The pKY241 plasmid contains a chloramphenicol resistance marker and the *gyrA* (amber) gene. *E. coli* KS40/pKY241 cells carrying the active *supF* gene are sensitive to nalidixic acid and form blue colonies on LB plates containing ampicillin, chloramphenicol, isopropyl-β-D-thiogalactopyranoside (IPTG), and 5-bromo-4-chloro-3-indolyl-β-D-galactopyranoside (X-gal), whereas cells carrying the mutated *supF* gene form white colonies on plates containing nalidixic acid, ampicillin, chloramphenicol, IPTG, and X-gal.

Construction of a shuttle vector plasmid containing an 8OHG residue

pMY189-8OHG, which is the shuttle plasmid pMY189 containing a single 8OHG:cytosine pair at nucleotide position 159 of the *supF* gene, was prepared according to a previously described method[30]. Briefly, *E. coli* XL1-Blue MRF' (Stratagene) and R408 Helper Phage (Stratagene) were used to prepare single-stranded pMY189 DNA, and 30 μg of the single-stranded pMY189 plasmid and a 5-fold molar excess of a 5'-phosphorylated 24-mer oligonucleotide with a single 8OHG at nucleotide position 159 of the *supF* gene [5'-CGA CTT CGA A (8OHG) G TTC GAA TCC TTC-3'] were annealed in a reaction mixture. Forty units of T4 DNA polymerase (New England Biolabs, Beverly, MA), 600 μmol/L of deoxynucleotide triphosphate (GE Healthcare Bio-Science), 36 Weiss units of T4 DNA ligase (New England Biolabs) and 1 mmol/L of ATP (Nacalai Tesque, Kyoto, Japan) were added to the

reaction mixture, and the mixture was incubated at 37 ℃ for 4 h. Closed circular pMY189-8OHG was isolated using cesium chloride-ethidium bromide density gradient centrifugation.

SupF forward mutation assay

Cells were cultured in the presence of cumate for 3 d for the induction of MUTYH expression, and they were then transfected with the shuttle plasmid pMY189 or pMY189-8OHG. After 48 h, the propagated plasmids were extracted from the cells using a QIAprep Spin Miniprep Kit (Qiagen, Valencia, CA) and digested with *Dpn*I restriction enzyme (New England Biolabs) to eliminate unreplicated plasmids with the bacterial methylation pattern. After purification with Amicon Ultra Centrifugal Filter Units (Millipore, Bedford, MA), the plasmids were introduced into the KS40/pKY241 indicator *E. coli* strain using electroporation. The transformants were plated onto LB agar plates containing 50 μg/mL of nalidixic acid, 150 μg/mL of ampicillin, and 30 μg/mL of chloramphenicol together with IPTG and X-gal. White colonies on were counted as *supF* mutants. The mutation frequencies were calculated as the number of *supF* mutants per the total number of transformants, which were counted on LB plates containing ampicillin, chloramphenicol, IPTG and X-gal.

Statistical analysis

The statistical analysis was performed using an unpaired *t*-test and JMP software, version 9 (SAS Institute, Cary, NC). *P*-values less than 0.05 were considered statistically significant.

RESULTS

Establishment of human cells inducibly expressing MUTYH variants

To investigate the ability of MUTYH variants to suppress mutations caused by 8OHG in human cells, we used the piggyBac transposon vector system[33] to establish human cells capable of inducibly expressing MUTYH variants and performed a *supF* forward mutation assay using the shuttle plasmid pMY189, which contains a single 8OHG in the *supF* gene. First, H1299 human cancer cells were transfected with a piggyBac cumate switch inducible vector for the expression of WT, p.R154H, p.M255V, p.L360P, or p.P377L MUTYH together with the piggyBac transposase vector; positively transposed cells were then selected with puromycin. We also transfected cells with an empty (parental) piggyBac cumate switch inducible vector and transposase vector. The expression of MUTYH protein after cumate induction was examined using Western blotting analysis using an anti-MUTYH monoclonal antibody (Figure 1A). MUTYH protein was abundantly expressed in cells in which a WT, p.R154H, p.M255V, p.L360P, or p.P377L MUTYH expression vector but not an empty vector was transposed. Immunofluorescence analysis also showed abundant MUTYH protein expression in cells in which a WT, p.R154H, p.M255V, p.L360P, or p.P377L MUTYH expression vector but not an empty vector was transposed (Figure 1B). In accordance with the previous finding that the MUTYH type 2 protein is the nuclear form[4,7], WT MUTYH protein was localized in the nucleus. All of the MUTYH variants were also localized in the nucleus, suggesting that the amino acid changes in p.R154H, p.M255V, p.L360P, and p.P377L did not alter the subcellular localization of these proteins in human cells. With regard to endogenous MUTYH expression, low levels were detected in the immunofluorescence analysis, as shown in the panel of empty vector-transposed cells (Figure 1B). When the intensity of the MUTYH protein signal was enhanced with image-editing software, the signal was observed in both the nucleus and cytoplasm (Figure 1C), which is compatible with the existence of both the type 1 mitochondrial form and the type 2 nuclear form[4,7]. Next, to confirm the nuclear localization of MUTYH type 2 variant forms, we constructed a vector to express MUTYH tagged with a FLAG peptide at the C-terminus and examined the localization of the MUTYH variants using immunofluorescence analysis with an anti-FLAG antibody (Figure 2). All of the variants showed nuclear localization, further suggesting that the amino acid changes in p.R154H, p.M255V, p.L360P, and p.P377L did not alter their subcellular localization in human cells. Together, the above findings indicate that human cells inducibly expressing the MUTYH variants (p.R154H, p.M255V, p.L360P, or p.P377L) and their control cells were properly prepared and were appropriate for evaluating the suppressive activities of MUTYH variants against oxidative mutagenesis in human cells.

Impaired activities of MUTYH variants in the suppression of oxidative mutagenesis in human cells in vivo

Next, mutation frequencies were compared for the empty vector-transposed human cells and the cumate-inducible stable cells expressing WT or variant MUTYH using a *supF* forward mutation assay with the shuttle plasmid pMY189. In this assay, we introduced a single 8OHG residue at position 159 of the *supF* gene in pMY189. The mutation frequency of *supF* was 2.2×10^{-2} in the 8OHG-containing pMY189 plasmid and 2.5×10^{-4} in WT pMY189 in empty vector-transposed cells (Figure 3), which was an 86-fold increase in mutation frequency with the introduction of 8OHG. The mutation frequency (4.7×10^{-3}) of *supF* in the 8OHG-containing pMY189 plasmid in cells overexpressing WT MUTYH was significantly lower than in the empty vector-transposed cells. However, the mutation frequencies of *supF* in the 8OHG-containing pMY189 plasmid in cells overexpressing the p.R154H, p.M255V, p.L360P, or p.P377L MUTYH variant were 1.84×10^{-2}, 1.55×10^{-2}, 1.91×10^{-2}, and 1.96×10^{-2}, respectively, meaning that no significant difference was observed in the mutation frequency between the empty vector-transposed cells and the cells overexpressing MUTYH variants. These results suggested that the suppressive activities of p.R154H, p.M255V, p.L360P,

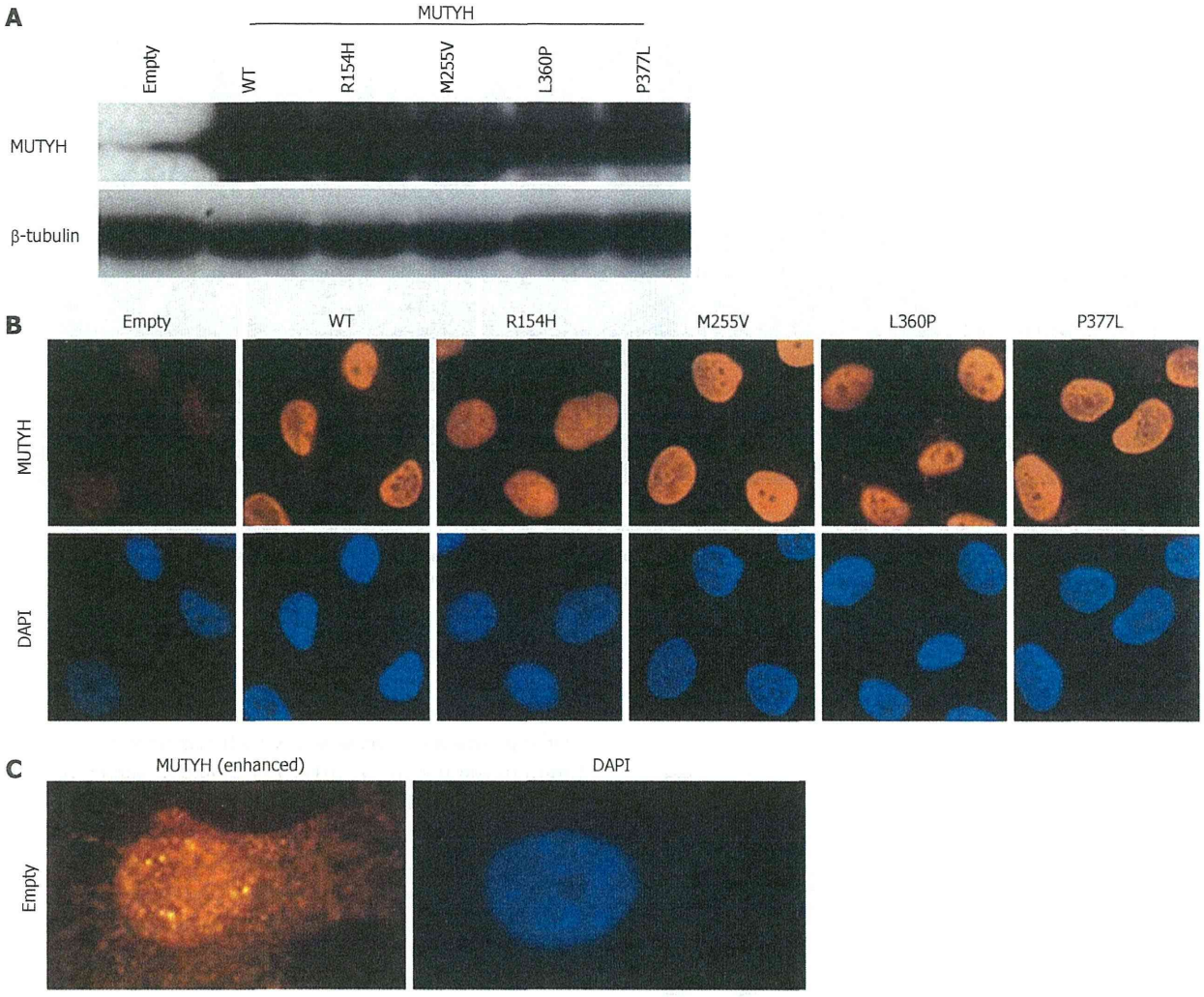

Figure 1 Establishment of H1299 human cell lines inducibly expressing MUTYH variant proteins. A: Detection of MUTYH proteins in cumate-inducible stable cell lines expressing MUTYH in the presence of cumate using Western blotting analysis with an anti-MUTYH antibody. Lysates from empty vector-transposed cells and cells inducibly expressing wild-type (WT) MUTYH or p.R154H, p.M255V, p.L360P, or p.P377L MUTYH variants were analyzed. β-tubulin protein was also analyzed as an internal control; B: Immunofluorescence detection of MUTYH proteins expressed in the cell lines used in (A) in the presence of cumate. The MUTYH protein (red) was stained with anti-MUTYH as the primary antibody and Alexa Fluor 594-conjugated goat anti-mouse IgG as the secondary antibody. The nuclei were counterstained with 4',6-diamidino-2-phenylindole (DAPI) (blue); C: Immunofluorescence detection of endogenous MUTYH proteins in the empty vector-transposed cells as described in (B). The intensity of the signals of MUTYH protein (red) was enhanced with image-editing software to determine the subcellular localization of endogenous MUTYH protein. The nuclei were counterstained with DAPI (blue).

and p.P377L MUTYH variants against mutations caused by 8OHG were severely impaired in human cells.

DISCUSSION

In this study, human cell lines inducibly expressing MUTYH variants (p.R154H, p.M255V, p.L360P, or p.P377L) were established, and the abilities of these cells to suppress mutations caused by 8OHG were compared using a *supF* forward mutation assay with a shuttle vector containing an 8OHG residue in the *supF* gene. The assay showed that the suppressive activities of p.R154H, p.M255V, p.L360P, and p.P377L MUTYH variants against mutations caused by 8OHG were severely impaired in human cells. To the best of our knowledge, this is the first analysis of the suppressive activities of MUTYH variants against oxidative mutagenesis in human cells *in vivo*.

The type 2 protein is the nuclear form of MUTYH[4,7], and somatic *APC* and *KRAS* (OMIM 190070) mutations occur in the nuclear DNA of MAP tumors[8,9,12]; therefore, we believed that it would be more appropriate to investigate type 2 rather than type 1 and we established cell lines expressing the type 2 form in this study. In the *supF* forward mutation assay using a shuttle vector containing 8OHG, no significant difference was observed in the mutation frequencies between empty vector-transposed cells and cells expressing 1 of the 4 MUTYH variants, indicating the severe impairment of the suppressive activities of the MUTYH variants against mutations caused by 8OHG in human cells *in vivo*. We previously showed that the adenine DNA glycosylase activity of the p.M255V protein was 10.7% of the level of the WT protein and that the DNA

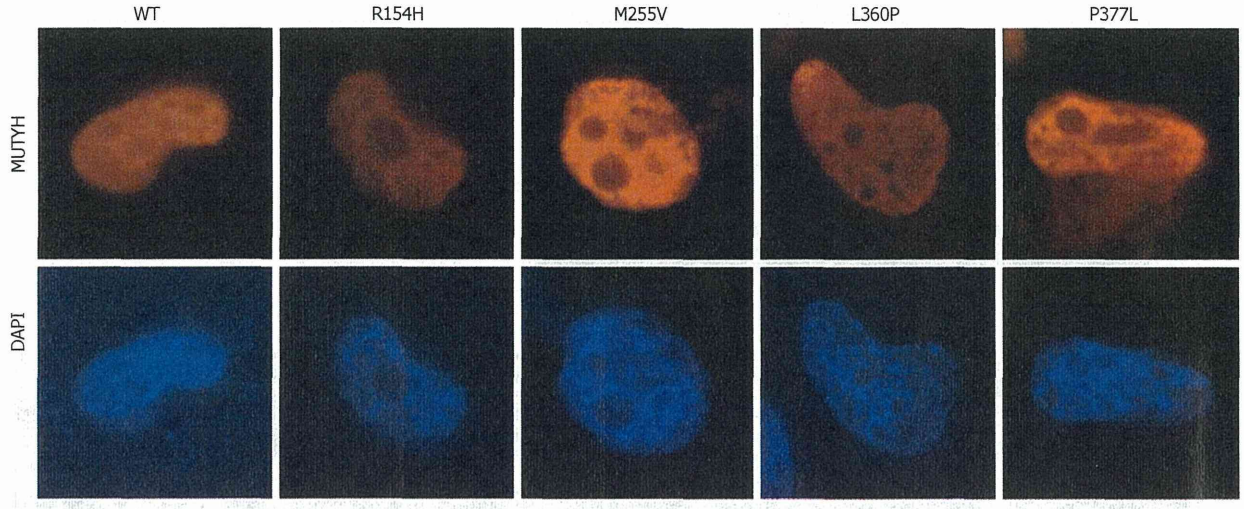

Figure 2 Nuclear localization of MUTYH variant proteins (p.R154H, p.M255V, p.L360P, and p.P377L). H1299 cells were transiently transfected with a vector expressing various types of MUTYH proteins tagged with FLAG, and MUTYH-FLAG protein (red) was stained with anti-FLAG M2 as the primary antibody and Alexa Fluor 594-conjugated goat anti-mouse IgG as the secondary antibody. The nuclei were counterstained with 4',6-diamidino-2-phenylindole (DAPI) (blue). WT: Wild-type.

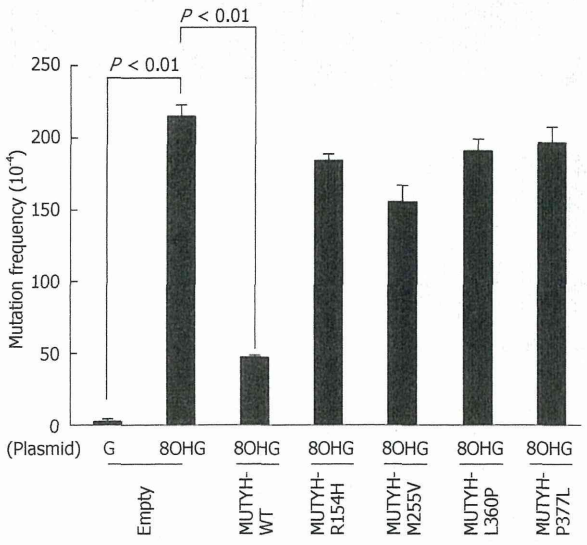

Figure 3 Measurement of the mutation frequency of the *supF* gene in the pMY189 plasmid using a *supF* forward mutation assay in H1299 human cell lines inducibly expressing MUTYH variant proteins. Empty vector-transposed cells and cells inducibly expressing wild-type (WT) MUTYH or p.R154H, p.M255V, p.L360P, or p.P377L MUTYH variants in the presence of cumate were transfected with a pMY189 shuttle plasmid, and the mutation frequency of *supF* in these human cell lines was measured. "8-hydroxyguanine (8OHG)" indicates a pMY189 plasmid containing an 8OHG residue at position 159 of *supF*, while "G" indicates a pMY189 plasmid containing the WT *supF* gene. The data are shown as the means ± SE.

glycosylase activities of the p.R154H, p.L360P, and p.P377L proteins were severely impaired[27]. Thus, the results regarding the regulation of the mutation frequency in the present study are in agreement with DNA glycosylase activity in the previous study. A combination of the results of two distinct analyses, i.e., *in vitro* and *in vivo* analyses, would provide more definitive proof of the pathogenicity of the p.R154H, p.M255V, p.L360P, and p.P377L MUTYH variants. Because the diagnosis of MAP depends on whether (1) the clinical phenotypic characteristics of MAP are present in a candidate patient; and (2) the repair activities of the MUTYH variants encoded in the two *MUTYH* alleles of the patient are decreased, even when gene variations are found in the patient by *MUTYH* mutation screening, information on the levels of the repair activities of MUTYH variants is indispensable for properly diagnosing MAP. Regarding this point, our results are clinically useful.

Previous studies have provided contradictory results regarding the subcellular localization of MUTYH protein in MAP patients; one paper insisted that MUTYH protein was predominantly localized in the cytoplasm of colorectal tumor cells in MAP patients but not in non-MAP patients, while the other papers denied this localization[34,35]. In the present study, the nuclear localization of the p.R154H, p.M255V, p.L360P, and p.P377L MUTYH type 2 variants was shown using two distinct experiments. Therefore, it seems that the amino acid changes of p.R154H, p.M255V, p.L360P, and p.P377L did not alter the subcellular localization of the MUTYH protein. Similarly, Molatore *et al*[26] recently reported that 3 missense MUTYH variants other than our variants were all localized in the nucleus.

In this paper, we successfully established cumate-inducible stable human cell lines by utilizing the piggyBac transposon vector system. Transposon technology is an attractive non-viral gene delivery model that allows for efficient genomic integration in a variety of cell types[36]. Among the several transposon systems available, the piggyBac transposon, which was isolated from the genome of the cabbage looper moth (*Trichoplusia ni*), has been optimized for gene transfer into mammalian cells[36,37]. In practice, the MUTYH expression status in our cell lines after puromycin selection in the presence of cumate clearly demonstrated abundant MUTYH expression in almost all of the cells. Because we performed transient transfection with a shuttle plasmid in the *supF* forward

mutation assay in this study, the genomic integration of the sequence for MUTYH expression using the piggyBac transposon system was well suited to our experiment.

In our experiments, the level of expression of exogenously introduced MUTYH was much higher than the level of expression of endogenous MUTYH. This scenario allowed us to effectively evaluate the activities of MUTYH variants to regulate the mutation frequency, and we believe that such an evaluation was successfully performed. However, we cannot completely exclude the possibility that the functional difference observed under experimental conditions of high MUTYH expression levels does not reflect a true functional difference.

The impaired activity of MUTYH variants was shown using H1299 human lung cancer cells in this study. We used this cell line because we believed that the ability of MUTYH variants to suppress mutations in H1299 cells is not different from their ability in human cells derived from the colorectum. If there are no organ type-specific systems to modulate MUTYH activity, then MUTYH activity is dependent on the MUTYH expression level and MUTYH variation. Moreover, we studied overexpressed and exogenous MUTYH variant proteins in this paper. Therefore, we believe our results can most likely be applied for colorectal cells. However, because it might be possible that the difference in organ type has an effect on the results of functional evaluation, we would like to evaluate this activity in human colorectal cells in the future.

Genetic screening for *MUTYH* mutations in the diagnosis of colorectal polyposis continues to be performed worldwide, and technological progress in genome sequencing analysis has contributed to efficient and rapid screening protocols. Therefore, increasing *MUTYH* nucleotide variants are likely to be detected in the future. For appropriate patient management, the levels of the repair activities of MUTYH variant proteins should be evaluated, and our system for determining the abilities of these variants to suppress oxidative mutagenesis in human cells *in vivo* may be of great use for such evaluations.

COMMENTS

Background

The *MUTYH* gene is responsible for MUTYH-associated polyposis (MAP), a relatively recently identified hereditary disease. Although 300 *MUTYH* variants have been found, only a small number of variants has been functionally characterized. Therefore, evaluations of the activities of MUTYH variant proteins are needed for the correct diagnosis of MAP.

Research frontiers

An *in vitro* DNA cleavage assay was performed to evaluate the repair activities of MUTYH variants. Despite the clinical importance of the multiplicity of functional analytical methods for evaluating the activities of MUTYH variant proteins, until now, the ability of MUTYH variants to suppress oxidative mutagenesis in human cells *in vivo* has not been previously analyzed.

Innovations and breakthroughs

Human cumate-inducible stable cell lines expressing various MUTYH variants were established using the piggyBac transposon vector system. This is the first report to utilize human cells expressing MUTYH variants encoded by an ectopically transposed gene. Moreover, this is the first report to analyze the suppressive activities of MUTYH variants against oxidative mutagenesis in human cells.

Applications

The results of the present study suggest that the suppressive activities of p.R154H, p.M255V, p.L360P, and p.P377L MUTYH variant proteins against mutations caused by 8-hydroxyguanine (8OHG) are severely impaired in human cells. These *in vivo* results combined with results from our previous *in vitro* analysis provide definitive proof of the pathogenicity of p.R154H, p.M255V, p.L360P, and p.P377L MUTYH variants. This conclusion is valuable for the appropriate diagnosis of MAP.

Terminology

The base excision repair protein MUTYH is involved in the repair of the oxidative base lesion 8OHG in DNA. Patients with biallelic inactivating germline mutations in the *MUTYH* gene are predisposed to MAP, which is characterized by the development of multiple colorectal adenomas and carcinomas.

Peer review

This is a good study in which authors analyze the suppressive activity of MUTYH variant proteins against mutations caused by 8OHG in human cells. Towards understanding the impact of having so many missense mutations among MAP patients, the authors have steadily developed an infrastructure for serving the patients in the future. Through expression of MUTYH WT and 4 variants, subcellular localization, and mutation frequency counting, they suggested that anti-mutation activity of the four MUTYH variants were severely impaired in human cells.

REFERENCES

1 **Kasai H**, Nishimura S. Hydroxylation of deoxyguanosine at the C-8 position by ascorbic acid and other reducing agents. *Nucleic Acids Res* 1984; **12**: 2137-2145

2 **Shibutani S**, Takeshita M, Grollman AP. Insertion of specific bases during DNA synthesis past the oxidation-damaged base 8-oxodG. *Nature* 1991; **349**: 431-434

3 **Slupska MM**, Luther WM, Chiang JH, Yang H, Miller JH. Functional expression of hMYH, a human homolog of the Escherichia coli MutY protein. *J Bacteriol* 1999; **181**: 6210-6213

4 **Takao M**, Zhang QM, Yonei S, Yasui A. Differential subcellular localization of human MutY homolog (hMYH) and the functional activity of adenine: 8-oxoguanine DNA glycosylase. *Nucleic Acids Res* 1999; **27**: 3638-3644

5 **Shinmura K**, Yamaguchi S, Saitoh T, Takeuchi-Sasaki M, Kim SR, Nohmi T, Yokota J. Adenine excisional repair function of MYH protein on the adenine: 8-hydroxyguanine base pair in double-stranded DNA. *Nucleic Acids Res* 2000; **28**: 4912-4918

6 **Tsai-Wu JJ**, Su HT, Wu YL, Hsu SM, Wu CH. Nuclear localization of the human mutY homologue hMYH. *J Cell Biochem* 2000; **77**: 666-677

7 **Ohtsubo T**, Nishioka K, Imaiso Y, Iwai S, Shimokawa H, Oda H, Fujiwara T, Nakabeppu Y. Identification of human MutY homolog (hMYH) as a repair enzyme for 2-hydroxyadenine in DNA and detection of multiple forms of hMYH located in nuclei and mitochondria. *Nucleic Acids Res* 2000; **28**: 1355-1364

8 **Al-Tassan N**, Chmiel NH, Maynard J, Fleming N, Livingston AL, Williams GT, Hodges AK, Davies DR, David SS, Sampson JR, Cheadle JP. Inherited variants of MYH associated with somatic G: C--> T: A mutations in colorectal tumors. *Nat Genet* 2002; **30**: 227-232

9 **Jones S**, Emmerson P, Maynard J, Best JM, Jordan S, Williams GT, Sampson JR, Cheadle JP. Biallelic germline mutations in MYH predispose to multiple colorectal adenoma and somatic G: C--> T: A mutations. *Hum Mol Genet* 2002; **11**: 2961-2967

10 **Sieber OM**, Lipton L, Crabtree M, Heinimann K, Fidalgo P, Phillips RK, Bisgaard ML, Orntoft TF, Aaltonen LA, Hodgson SV, Thomas HJ, Tomlinson IP. Multiple colorectal adenomas, classic adenomatous polyposis, and germ-line mutations in MYH. *N Engl J Med* 2003; **348**: 791-799

11 **Sampson JR**, Dolwani S, Jones S, Eccles D, Ellis A, Evans DG, Frayling I, Jordan S, Maher ER, Mak T, Maynard J, Pi-

gatto F, Shaw J, Cheadle JP. Autosomal recessive colorectal adenomatous polyposis due to inherited mutations of MYH. *Lancet* 2003; **362**: 39-41

12 **Lipton L**, Halford SE, Johnson V, Novelli MR, Jones A, Cummings C, Barclay E, Sieber O, Sadat A, Bisgaard ML, Hodgson SV, Aaltonen LA, Thomas HJ, Tomlinson IP. Carcinogenesis in MYH-associated polyposis follows a distinct genetic pathway. *Cancer Res* 2003; **63**: 7595-7599

13 **Nielsen M**, Morreau H, Vasen HF, Hes FJ. MUTYH-associated polyposis (MAP). *Crit Rev Oncol Hematol* 2011; **79**: 1-16

14 **Sheng JQ**, Cui WJ, Fu L, Jin P, Han Y, Li SJ, Fan RY, Li AQ, Zhang MZ, Li SR. APC gene mutations in Chinese familial adenomatous polyposis patients. *World J Gastroenterol* 2010; **16**: 1522-1526

15 **Out AA**, Tops CM, Nielsen M, Weiss MM, van Minderhout IJ, Fokkema IF, Buisine MP, Claes K, Colas C, Fodde R, Fostira F, Franken PF, Gaustadnes M, Heinimann K, Hodgson SV, Hogervorst FB, Holinski-Feder E, Lagerstedt-Robinson K, Olschwang S, van den Ouweland AM, Redeker EJ, Scott RJ, Vankeirsbilck B, Grønlund RV, Wijnen JT, Wikman FP, Aretz S, Sampson JR, Devilee P, den Dunnen JT, Hes FJ. Leiden Open Variation Database of the MUTYH gene. *Hum Mutat* 2010; **31**: 1205-1215

16 **Shinmura K**, Yamaguchi S, Saitoh T, Kohno T, Yokota J. Somatic mutations and single nucleotide polymorphisms of base excision repair genes involved in the repair of 8-hydroxyguanine in damaged DNA. *Cancer Lett* 2001; **166**: 65-69

17 **Yamaguchi S**, Shinmura K, Saitoh T, Takenoshita S, Kuwano H, Yokota J. A single nucleotide polymorphism at the splice donor site of the human MYH base excision repair genes results in reduced translation efficiency of its transcripts. *Genes Cells* 2002; **7**: 461-474

18 **Wooden SH**, Bassett HM, Wood TG, McCullough AK. Identification of critical residues required for the mutation avoidance function of human MutY (hMYH) and implications in colorectal cancer. *Cancer Lett* 2004; **205**: 89-95

19 **Bai H**, Jones S, Guan X, Wilson TM, Sampson JR, Cheadle JP, Lu AL. Functional characterization of two human MutY homolog (hMYH) missense mutations (R227W and V232F) that lie within the putative hMSH6 binding domain and are associated with hMYH polyposis. *Nucleic Acids Res* 2005; **33**: 597-604

20 **Parker AR**, Sieber OM, Shi C, Hua L, Takao M, Tomlinson IP, Eshleman JR. Cells with pathogenic biallelic mutations in the human MUTYH gene are defective in DNA damage binding and repair. *Carcinogenesis* 2005; **26**: 2010-2018

21 **Bai H**, Grist S, Gardner J, Suthers G, Wilson TM, Lu AL. Functional characterization of human MutY homolog (hMYH) missense mutation (R231L) that is linked with hMYH-associated polyposis. *Cancer Lett* 2007; **250**: 74-81

22 **Yanaru-Fujisawa R**, Matsumoto T, Ushijima Y, Esaki M, Hirahashi M, Gushima M, Yao T, Nakabeppu Y, Iida M. Genomic and functional analyses of MUTYH in Japanese patients with adenomatous polyposis. *Clin Genet* 2008; **73**: 545-553

23 **Ali M**, Kim H, Cleary S, Cupples C, Gallinger S, Bristow R. Characterization of mutant MUTYH proteins associated with familial colorectal cancer. *Gastroenterology* 2008; **135**: 499-507

24 **Kundu S**, Brinkmeyer MK, Livingston AL, David SS. Adenine removal activity and bacterial complementation with the human MutY homologue (MUTYH) and Y165C, G382D, P391L and Q324R variants associated with colorectal cancer. *DNA Repair (Amst)* 2009; **8**: 1400-1410

25 **Forsbring M**, Vik ES, Dalhus B, Karlsen TH, Bergquist A, Schrumpf E, Bjørås M, Boberg KM, Alseth I. Catalytically impaired hMYH and NEIL1 mutant proteins identified in patients with primary sclerosing cholangitis and cholangiocarcinoma. *Carcinogenesis* 2009; **30**: 1147-1154

26 **Molatore S**, Russo MT, D'Agostino VG, Barone F, Matsumoto Y, Albertini AM, Minoprio A, Degan P, Mazzei F, Bignami M, Ranzani GN. MUTYH mutations associated with familial adenomatous polyposis: functional characterization by a mammalian cell-based assay. *Hum Mutat* 2010; **31**: 159-166

27 **Goto M**, Shinmura K, Nakabeppu Y, Tao H, Yamada H, Tsuneyoshi T, Sugimura H. Adenine DNA glycosylase activity of 14 human MutY homolog (MUTYH) variant proteins found in patients with colorectal polyposis and cancer. *Hum Mutat* 2010; **31**: E1861-E1874

28 **Yamane A**, Shinmura K, Sunaga N, Saitoh T, Yamaguchi S, Shinmura Y, Yoshimura K, Murakami H, Nojima Y, Kohno T, Yokota J. Suppressive activities of OGG1 and MYH proteins against G: C to T: A mutations caused by 8-hydroxyguanine but not by benzo[a]pyrene diol epoxide in human cells in vivo. *Carcinogenesis* 2003; **24**: 1031-1037

29 **Suzuki T**, Harashima H, Kamiya H. Effects of base excision repair proteins on mutagenesis by 8-oxo-7,8-dihydroguanine (8-hydroxyguanine) paired with cytosine and adenine. *DNA Repair (Amst)* 2010; **9**: 542-550

30 **Shinmura K**, Goto M, Suzuki M, Tao H, Yamada H, Igarashi H, Matsuura S, Maeda M, Konno H, Matsuda T, Sugimura H. Reduced expression of MUTYH with suppressive activity against mutations caused by 8-hydroxyguanine is a novel predictor of a poor prognosis in human gastric cancer. *J Pathol* 2011; **225**: 414-423

31 **Tao H**, Shinmura K, Hanaoka T, Natsukawa S, Shaura K, Koizumi Y, Kasuga Y, Ozawa T, Tsujinaka T, Li Z, Yamaguchi S, Yokota J, Sugimura H, Tsugane S. A novel splice-site variant of the base excision repair gene MYH is associated with production of an aberrant mRNA transcript encoding a truncated MYH protein not localized in the nucleus. *Carcinogenesis* 2004; **25**: 1859-1866

32 **Matsuda T**, Yagi T, Kawanishi M, Matsui S, Takebe H. Molecular analysis of mutations induced by 2-chloroacetaldehyde, the ultimate carcinogenic form of vinyl chloride, in human cells using shuttle vectors. *Carcinogenesis* 1995; **16**: 2389-2394

33 **Ding S**, Wu X, Li G, Han M, Zhuang Y, Xu T. Efficient transposition of the piggyBac (PB) transposon in mammalian cells and mice. *Cell* 2005; **122**: 473-483

34 **Di Gregorio C**, Frattini M, Maffei S, Ponti G, Losi L, Pedroni M, Venesio T, Bertario L, Varesco L, Risio M, Ponz de Leon M. Immunohistochemical expression of MYH protein can be used to identify patients with MYH-associated polyposis. *Gastroenterology* 2006; **131**: 439-444

35 **van der Post RS**, Kets CM, Ligtenberg MJ, van Krieken JH, Hoogerbrugge N. Immunohistochemistry is not an accurate first step towards the molecular diagnosis of MUTYH-associated polyposis. *Virchows Arch* 2009; **454**: 25-29

36 **Macdonald J**, Taylor L, Sherman A, Kawakami K, Takahashi Y, Sang HM, McGrew MJ. Efficient genetic modification and germ-line transmission of primordial germ cells using piggyBac and Tol2 transposons. *Proc Natl Acad Sci USA* 2012; **109**: E1466-E1472

37 **Cary LC**, Goebel M, Corsaro BG, Wang HG, Rosen E, Fraser MJ. Transposon mutagenesis of baculoviruses: analysis of Trichoplusia ni transposon IFP2 insertions within the FP-locus of nuclear polyhedrosis viruses. *Virology* 1989; **172**: 156-169

S- Editor Gou SX **L- Editor** A **E- Editor** Zhang DN

Phosphorus, Sulfur, and Silicon, 188:213–223, 2013

ISSN: 1042-6507 print / 1563-5325 online
DOI: 10.1080/10426507.2012.744016

RESEARCH ON PHOSPHA SUGAR ANALOGUES TO DEVELOP NOVEL MULTIPLE TYPE MOLECULAR TARGETED ANTITUMOR DRUGS AGAINST VARIOUS TYPES OF TUMOR CELLS

Reiko Makita,[1] Mitsuji Yamashita,[1] Michio Fujie,[2] Mayumi Yamaoka,[3] Keita Kiyofuji,[1] Manabu Yamada,[1] Junko Yamashita,[1] Kenji Tsunekawa,[1] Kazuhide Asai,[3] Takuya Suyama,[3] Mitsuo Toda,[3] Yasutaka Tanaka,[3] Haruhiko Sugimura,[2] Yasuhiro Magata,[2] Kazunori Ohnishi,[2] and Satoki Nakamura[2]

[1]*Department of Nano Materials, Graduate School of Science and Technology, Shizuoka University, Hamamatsu, Japan*
[2]*Faculty of Medicine, Hamamatsu University School of Medicine, Hamamatsu, Japan*
[3]*Department of Materials Science, Graduate School of Engineering, Shizuoka University, Hamamatsu, Japan*

GRAPHICAL ABSTRACT

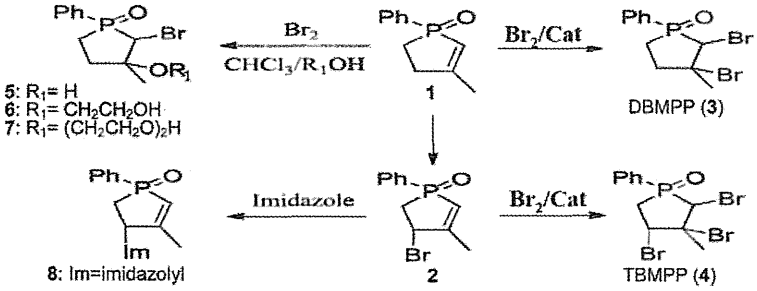

Preparation of phospha sugar derivatives **2–8** from 2-phospholene 1.

Abstract *The synthesis and antitumor activity evaluation of new branched phospha sugars, especially deoxybromophospha sugar derivatives or bromophospholanes of 2,3-dibromo-3-methyl-1-phenylphospholane 1-oxide (DBMPP: 3) and 2,3,4-tribromo-3-methyl-1-phenylphospholane 1-oxide (TBMPP: 4), against various types of leukemia cell lines as well*

Received 15 September 2012; accepted 23 October 2012.
The authors greatly acknowledge financial supports by Satellite Shizuoka and the Headquarters of Japan Science and Technology Agency (JST) and Grant-in-Aid for Scientific Research by Japan Society for the Promotion of Science (JSPS) (Grant 19650112, 21650108) and Ministry of Education, Culture, Sports, Science and Technology (MEXT) (H19-Nano-Ippan-015), and Sugiyama Kohokai Foundation.
Address correspondence to Mitsuji Yamashita, Department of Nano Materials, Graduate School of Science and Technology, Shizuoka University, Johoku 3-5-1, Naka-ku, Hamamatsu 432-8011, Japan. E-mail: tcmyama@ipc.shizuoka.ac.jp

*as the results of the mechanistic studies for characterizing and developing the novel multiple type molecular targeted antitumor agents are reported in this paper. DBMPP and TBMPP were prepared from 1-phenyl-3-methyl-2-phospholene 1-oxide (**1**). The isomer mixture of phospha sugars prepared were evaluated as novel antitumor agents by MTT in vitro method. DBMPP and TBMPP were characterized by flow cytometry and Western blot analysis and were revealed to be potential antitumor agents against leukemia cell lines of K562 (one type of leukemia cell lines of CML) and U937 (one type of leukemia cell lines of AML) as well as against the various types of leukemia cell lines and also against solid tumor cell lines of stomach, skin, and lung cancers by MTT evaluation and observation by a handstand phase-contrast microscope. The results of the flow cytometry indicated that the mechanism of apoptosis induced by phospha sugar derivatives not only to tumor cells of leukemia cell lines of U937 but also to tumor cells of various kinds of leukemia cell lines selectively to decrease the tumor cell viability of various kinds of leukemia cell lines. The Western blot analyses for phospha sugar DBMPP against U937 leukemia cell lines showed that the phospha sugar affected on the expressions of the factors of cell cycles in the manners of suppressing the expression of the accelerator factors of cell cycles of tumor cells and enhancing the expression of suppressor factors of cell cycles of tumor cells by the medications of phospha sugars. TBMPP enhanced the expression of IER5 and then suppressed the expression of Cdc25B, which is the common factor to accelerate the cell cycles of various kinds of tumor cells. Therefore, suppression of the expression of Cdc25B by TBMPP implies that the branched deoxybromophospha sugar derivatives might be novel and potential multiple type molecular targeted antitumor agents against various kinds of tumor cell lines.*

Keywords Phosphorus heterocycles; branched deoxybromophospha sugars; molecular targeted antitumor agents; MTT *in vitro* evaluation; flow cytmetry; Western blot analysis

INTRODUCTION

Well known typical pseudo sugars are *carba*-, *aza*-, and *thia*-sugars,[1–4] which have a carbon–carbon–carbon, carbon–nitrogen–carbon, or carbon–sulfur–carbon linkage, respectively, instead of the carbon–oxygen–carbon linkage in the hemiacetal ring of the normal sugars. These pseudo sugars are known to exist in nature and are also chemically prepared by applying methodologies of synthetic sugar chemistry, where common sugars are generally used as the starting materials, for synthesizing pseudo sugars via a series of reactions of protection of specific hydroxyl groups, carbon-hetero atom bond formation, deprotection, and finally formation of the heterocycles by the reconstruction of the hemiacetal ring of sugars.[5] Pseudo sugars are known to exert important biological activities, therefore, many studies on not only the isolation and synthesis of the pseudo sugars but also on the characterization and evaluation of the biological activities are actively performed and reported.[6–9] On the other hand, phospha sugars, being classified into one new category of the pseudo sugars having the carbon–phosphorus–carbon linkage in the hemiacetal ring of sugars, are not yet found in nature and the syntheses of them are rather difficult compared with the typical pseudo sugars such as *aza*- and *thia*-sugars.[4,5,10–12]

We have been searching biologically active phospha sugars and we have first found new phospha sugar derivatives which provided good antitumor activities against leukemia cell lines by *in vitro* evaluation of 3-(4,5-dimethylthiazol-2-yl)-2,5-diphenyl-2*H*-tetrazolium bromide (MTT) methods.[13] In this paper we will deal with the successful preparation of branched phospha sugars including deoxybromophospha sugars of

2,3-dibromo-3-methyl-1-phenylphospholane 1-oxide (DBMPP: **3**) and 2,3,4-tribromo-3-methyl-1-phenylphospholene 1-oxide (TBMPP: **4**). The evaluations and characterizations of the DBMPP and TBMPP by the MTT method and the Western blot analysis revealed that phospha sugars have excellent characters as antitumor agents with high activities, wide spectra, good selectivity, and specificity against various kinds of leukemia cell lines. Western blot analysis for DBMPP and TBMPP against leukemia cell lines showed that DBMPP suppressed the expression of several tumor cell cycle accelerators and enhanced the expression of tumor cell cycle suppressors. TBMPP enhanced the expression of IER5 and then suppressed the expression of Cdc25B.

RESULTS AND DISCUSSION

Synthesis of Phospha Sugar Derivatives

Branched deoxypbromophospha sugar derivatives of 2,3-dibromo-3-methyl-1-phenylphospholane 1-oxide (DBMPP: **3**) and 2,3,4-tribromo-3-methyl-1-phenylphospholane 1-oxide (TBMPP: **4**) were prepared from the starting material of 3-methyl-1-phenyl-2-phospholene 1-oxide (**1**) and 4-bromo-3-methyl-1-phenyl-2-phopholene 1-oxide (**2**) as shown in Scheme 1.[12] Here, DBMPP (**3**) and TBMPP (**4**) were prepared by simple and efficient synthetic methods by addition of bromine to the C=C double bond of the 2-phospholenes **1** and **2** with or without catalyst in yields of 90% and 69%, respectively. Deoxybromophospha sugar derivatives with oxygen functionalities OR_1 (**5** (R_1 = H), **6** (R_1 = CH_2CH_2OH), and **7** (R_1 = $(CH_2CH_2O)_2H$)) on the 3-position were prepared by the reaction of **1** with bromine in the presence of water, ethylene glycol, and diethylene glycol, respectively, in yields of 55%, 88%, and 58%. 4-Imidazolyl derivative **8** was prepared from 4-bromo derivative **2** by the substitution reaction of the 4-bromo group by imidazole in a yield of 93% (Scheme 1).

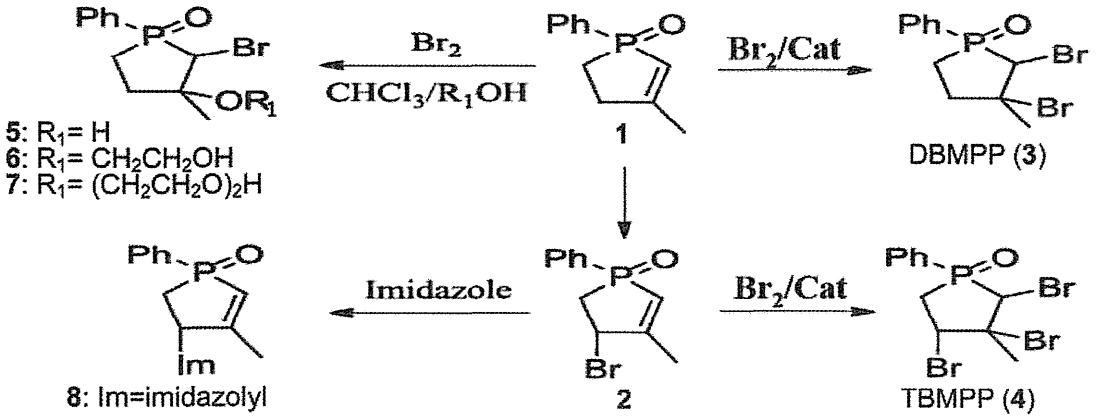

Scheme 1 Preparation of phospha sugar derivatives **2–8** from 2-phospholene 1.

Antitumor Activity and Cell Cycle Analysis[13,14]

Antitumor activity for the prepared phospha sugar derivatives **2–8** was evaluated by MTT *in vitro* method against K562 and U937 cell lines, whose results of antitumor activities are summarized in Table 1. Among these branched phospha sugar derivatives, bromo derivatives were active, especially DBMPP (**3**) and TBMPP (**4**) were quite active,